



LINKAGE BETWEEN THE FREQUENCY OF  
TROPICAL CYCLONES IN THE  
SOUTHWESTERN INDIAN OCEAN TO THE  
RAINFALL IN KENYA DURING THE MARCH  
TO MAY SEASON

**BY**

**FRANCIS MASINDE WAKACHALA**

**I56/12005/2018**

**THE DISSERTATION HAS BEEN SUBMITTED IN PARTIAL FULFILLMENT OF THE  
REQUIREMENTS FOR THE DEGREE OF MASTER OF SCIENCE IN METEOROLOGY OF  
THE UNIVERSITY OF NAIROBI**

**UNIVERSITY OF NAIROBI**

**DEPARTMENT OF EARTH AND CLIMATE SCIENCE**

**JULY, 2023**

**DECLARATION**

I declare that this Dissertation is my original work and has not been submitted elsewhere for research. Where other people’s work has been used, this has properly been acknowledged and referenced in accordance with the University of Nairobi’s requirements


Signature. 

Date.27/11/2023.

Francis Masinde Wakachala

I56/12005/2018

This dissertation has been submitted for evaluation with our endorsement as University Supervisors:


Signature... 

..... Date...12/1/2023.....

Prof. Franklin J. Opijah

Department of Earth and Climate science

University of Nairobi

Signature... 

.. Date...12-1-2023.....

Prof. Joseph N. Mutemi

Department of Earth and Climate science

University of Nairobi

## **DEDICATION**

I dedicate this dissertation to my parents, relatives, siblings, and friends for their unwavering support during my academic journey.

## ACKNOWLEDGEMENT

I express gratitude to God for his benevolence and the fortitude he granted me, enabling me to successfully complete my degree programme. Furthermore, I would like to convey my appreciation to my supervisors, Professor Franklin Opijah and Professor Joseph Mutemi, for their exemplary guidance, motivation, and expert guidance throughout the entire duration of my dissertation research. Without their aid, I would have had considerable difficulty completing my dissertation. The Kenya Meteorological Department expresses gratitude to the Ministry of Environment, Climate Change, and Forestry for obtaining permission to conduct a study. I would like to extend my appreciation to the staff of the Meteorological Department for their unwavering assistance during my academic journey. Furthermore, I would like to convey my gratitude to my colleagues at the meteorological station located at Kisumu International Airport. I would like to express my gratitude to the technical and support staff members in the Earth and Climate Science department at the Meteorological Office on the Chiromo Campus for their valuable assistance and support.

Finally, I would like to express my appreciation to my fellow students for their consistent presence and helpfulness whenever it was needed, as well as to my friends who provided aid in many ways.

## ABSTRACT

The economic activities in Kenya are heavily reliant on rainfall, particularly during the primary rainy season which occurs from March to May. This study investigates the relationship between the extended rainy season (March–April–May) and the frequency of tropical cyclones in the Southwestern Indian Ocean (SWIO). It examines monthly tropical cyclone frequency in the SWIO from November 1979 to April 2019 as well as MAM rainfall data from 1980 to 2019. To investigate the distribution of MAM rains in Kenya, time series and spatial maps were analyzed. The statistical significance was evaluated using the Student test, the trend's seasonal significance was ascertained using the Mann-Kendall trend test, and the percentage deviation from the norm was measured using coefficients of variation. Subsequently, the Taylor diagram was employed to conduct correlation analysis. The coefficient of variation calculation reveals that arid and semi-arid lands (ASALs) are exceptionally susceptible to their significant fluctuation throughout the March–April–May season, which is characterized by unreliable signals across all zones. Based on Mann-Kendall analysis, the seasonal rainfall trend is insignificant in eleven out of the twelve homogenous zones. There has been a significant change in the trend of Zone 2 (Moyale Station). Tropical storm occurrences in the Southwest Indian Ocean shown a slight inverse correlation with long-term seasonal precipitation in the majority of areas. The analysis of long-term MAM rainfall, in comparison to the MAM seasons of 2006 and 2019, reveals that the 2019 MAM season exhibits a negative deviation across all zones due to a significant occurrence of cyclones. In contrast, the 2006 MAM season exhibits a positive deviation from the average as a result of more rainfall in most uniform zones and a lower number of documented tropical cyclones. An important examination demonstrated a strong correlation between tropical cyclones and seven out of the twelve homogeneous zones. Tropical storm occurrences in the southern Indian Ocean adversely affect Kenya's long rain season. Further investigation is required to ascertain the impact of tropical cyclone intensities on the daily, weekly, and decadal patterns of rainfall and its distribution during the season.

## TABLE OF CONTENTS

|   |            |
|---|------------|
| <b>DECLARATION.....</b>                               | <b>ii</b>  |
| <b>DEDICATION.....</b>                                | <b>iii</b> |
| <b>ACKNOWLEDGEMENT.....</b>                           | <b>iv</b>  |
| <b>ABSTRACT.....</b>                                  | <b>v</b>   |
| <b>LIST OF FIGURES .....</b>                          | <b>ix</b>  |
| <b>LIST OF TABLES .....</b>                           | <b>xi</b>  |
| <b>ABBREVIATIONS AND ACRONYMS.....</b>                | <b>xii</b> |
| <b>LIST OF SYMBOLS .....</b>                          | <b>xv</b>  |
| <b>1      CHAPTER ONE: INTRODUCTION .....</b>         | <b>1</b>   |
| 1.0      Background .....                             | 1          |
| 1.1      Statement of Problem.....                    | 3          |
| 1.2      Research Questions .....                     | 3          |
| 1.3      Objectives.....                              | 3          |
| 1.4      Justification .....                          | 4          |
| 1.5      Area of study .....                          | 5          |
| 1.5.1    Location.....                                | 5          |
| 1.5.2    Weather and Climate of Kenya .....           | 6          |
| 1.5.3    Systems Influencing Rainfall over Kenya..... | 7          |
| 1.5.3.1   Inter-Tropical Convergence Zone .....       | 8          |
| <b>2      CHAPTER TWO: LITERATURE REVIEW .....</b>    | <b>13</b>  |
| 2.0      Introduction .....                           | 13         |
| 2.1      Rainfall Variability.....                    | 13         |
| <b>3      CHAPTER THREE .....</b>                     | <b>19</b>  |
| 3.0      DATA AND METHODOLOGY .....                   | 19         |
| 3.1      Types and Sources of Data.....               | 19         |

|          |   |           |
|----------|---|-----------|
| 3.1.1    | Observed Historical Rainfall Data .....   | 19        |
| 3.1.2    | Tropical Cyclone Data .....   | 20        |
| 3.1.3    | Data Quality Control .....  | 20        |
| 3.2      | METHODOLOGY.....  | 22        |
| 3.2.1    | Assessment of the Spatial and Temporal Patterns of MAM Seasonal Rainfall in Kenya<br>22   |           |
| 3.2.2    | Determining Intra-Seasonal Variability and Trends in the Frequency of Tropical<br>Cyclones North of 20°S and West of 60°E in the SWIO Region .....                    | 26        |
| 3.2.3    | Examination of the Potential Linkage of Frequency occurrence of Tropical Cyclones<br>over SWIO region and MAM Seasonal Rainfall Kenya.....                            | 26        |
| <b>4</b> | <b>CHAPTER FOUR.....</b>  | <b>31</b> |
| 4.0      | RESULTS AND DISCUSSION .....  | 31        |
| 4.1      | Results from Data Quality.....  | 31        |
| 4.2      | Determination of Spatial and Temporal Distribution in MAM Seasonal Rains of<br>Homogeneous Zones in Kenya .....   | 32        |
| 4.2.1    | Spatial Distribution of MAM Seasonal Rains of the Homogeneous Zones in Kenya ...  | 32        |
| 4.2.2    | Temporal distribution of MAM seasonal rainfall data for homogeneous zones in Kenya<br>34  |           |
| 4.3      | Determining the Intra-Seasonal Variability and Tendencies in the Frequency occurrence<br>of Tropical Cyclones North of 20°S and West of 60°E in the SWIO Region ..... | 38        |
| 4.3.1    | Determining the Trends and the Intra-Seasonal Variability of Tropical Cyclones.....   | 38        |
| 4.3.2    | Temporal Variability and Trends in MAM Seasonal Precipitation .....   | 41        |
| 4.3.3    | The Coefficient of Variation in MAM seasonal Rainfall in Kenya .....  | 43        |
| 4.4      | Examination of the Potential Linkage of Frequency occurrence of Tropical Cyclones<br>over SWIO region and MAM Seasonal Rainfall Kenya.....                            | 45        |
| 4.4.1    | Temporal Distribution of Tropical Cyclone and MAM Rainfall .....  | 46        |
| 4.4.2    | Examine link of Tropical Cyclone occurrence over the southwestern of the Indian<br>Ocean region to March-April-May Seasonal Rainfall in Kenya .....                   | 48        |

|          |  |           |
|----------|--|-----------|
| 4.4.3    | Link between the extreme occurrence of Tropical Cyclones over southwestern of Indian Ocean and the performance during the 2006 and 2019 March-April-May Seasons..... | 54        |
| 4.4.4    | The Spatial Characteristics of the Long-Term Mean of MAM Rainfall and the Seasonal Rains for MAM 2006 and 2019 .....   | 58        |
| <b>5</b> | <b>CHAPTER FIVE.....</b>   | <b>60</b> |
| 5.0      | CONCLUSIONS AND RECOMMENDATIONS .....  | 60        |
| 5.1      | Conclusions .....  | 60        |
| 5.2      | Recommendations .....  | 62        |
| 5.2.1    | To Scientists .....  | 62        |
| 5.2.2    | To Policymakers.....   | 63        |
| 5.2.3    | To Users .....   | 63        |
|          | <b>REFERENCES.....</b>   | <b>64</b> |
|          | <b>APPENDIX.....</b>   | <b>76</b> |



## LIST OF FIGURES

|  |    |
|--|----|
| Figure 1-1: Map of area of study showing the topographic elevation (m), and the representative rainfall stations and its location in Africa .....  | 6  |
| Figure 3-1: Homogeneous rainfall zones for Kenya's Mar-Apr-May (MAM) season .....  | 19 |
| Figure 3-2: The Taylor diagram is depicted schematically for estimating standard deviation, root mean square error (RMSE), and Pearson correlation. ....   | 28 |
| Figure 4-1: Single mass curves of cumulative MAM rainfall for homogeneous rainfall zones 2,6 and 10 of Kenya .....   | 31 |
| Figure 4-2: Single mass curves of cumulative MAM rainfall for homogeneous rainfall zones 5,8 and 12 of Kenya .....   | 32 |
| Figure 4-3: The spatial distribution of precipitation (measured in millimeters) in Kenya during the March-April (MAM) season from 1980 to 2020 is depicted. Regions with the highest amount of rainfall are indicated by the deep blue color, while places with the lowest amount are represented by brown. .... | 34 |
| Figure 4-4: Rainfall anomalies during the March-April-May season were examined for three Kenyan stations: Lodwar, Moyale, and Wajir, from 1980 to 2019. Zone 1, Zone 2, and Zone 3 are represented by these stations.....  | 35 |
| Figure 4-5: Rainfall anomalies for the March-April-May season between 1980 to 2019 for Garissa, Lamu and Moi international airport station representing zone4, zone 5 and zone 6 in Kenya ....   | 36 |
| Figure 4-6: The rainfall anomalies during the March-April-May season from 1980 to 2019 were analyzed for three stations in Kenya, namely Voi, Dagoretti corner, and Nanyuki. These stations represent Zone 7, Zone 8, and Zone 9, respectively. ....   | 37 |
| Figure 4-7: Rainfall anomalies for the March-April-May season between 1980 to 2019 for stations representing the homogeneous rainfall zones in Kenya .....   | 38 |
| Figure 4-8: Cyclone frequency variation over the Southwestern of the Indian Ocean for the period 1980-2019 .....   | 40 |
| Figure 4-9: Cyclone frequency trend and inter-annual variation of tropical cyclones over SWIO from 1980 to 2019.....   | 41 |
| Figure 4-10: Spatial distribution of Coefficient of Variation in percentage (%) of the March-April-May rains over Kenya based on data, 1979-2019.....  | 45 |
| Figure 4-11: Time series graphs shows the tropical cyclone occurrence in March over the SWIO with the MAM seasonal rainfall for homogeneous Zones.....   | 46 |

|  |    |
|--|----|
| Figure 4-12: Time series graphs shows the Tropical Cyclone occurrence (TCs seasonal occurrence) over the SWIO against the MAM seasonal rainfall for homogeneous Zones. ....  | 48 |
| Figure 4-13: The Taylor diagram illustrates the Pearson correlation, root mean square error, and standard deviation between the occurrence of tropical cyclones in February and the seasonal rainfall in Kenya during March, April, and May.. .... | 49 |
| Figure 4-14: Taylor diagram displaying the Pearson correlation, root mean square error, and standard deviation between March tropical cyclone with the March-April-May seasonal rainfall in Kenya. ....  | 50 |
| Figure 4-15: Taylor diagram displaying the Pearson correlation, root mean square error, and standard deviation between Seasonal Tropical Cyclones and March-April-May seasonal rainfall in Kenya. ....   | 52 |
| Figure 4-16: The spatial distribution of percentage deviation of the MAM seasonal rainfall of 2006 and 2019 over Kenya .....   | 57 |
| Figure 4-17: The spatial distribution of Long Term Mean of March-April-May season (1980-2019) (a), 2006 March-April-May season (b) and 2019 March-April-May season (c) of Kenya .....  | 59 |

## LIST OF TABLES

|   |    |
|---|----|
| Table 3-1: Tabular display of Synoptic Rainfall Stations with Latitude, Longitude, Elevation, and Long Term Mean of MAM Seasonal Rainfall over the research area..... | 20 |
| Table 4-1: Tropical cyclone occurrence over the Southwestern of the Indian Ocean, 1979-201939   |    |
| Table 4-2: Tabulation of p-value and Kendall rank correlation (Tau) using seasonal rainfall for the 12 homogenous zones of Kenya .....                                | 42 |
| Table 4-3: Mean, standard deviation, and coefficient of variation of rainfall over Kenya for the March-April-May season .....   | 44 |
| Table 4-4: the calculated correlation and Student tests result showing t test and p-values .....  | 54 |
| Table 4-5:: Comparison between MAM long term mean (LTM) rainfall, MAM of 2006 and the MAM of 2019 season.....   | 56 |

## ABBREVIATIONS AND ACRONYMS

|                   |       |  |
|-------------------|-------|--|
| ACE               | ----- | Accumulated cyclone energy                                 |
| ARB               | ----- | Arabian Sea  |
| ASAL              | ----- | Arid and Semi-Arid Lands                                   |
| BoB               | ----- | Bay of Bengal  |
| CIMSS             | ----- | Cooperative Institute for Meteorological Satellite Studies |
| CS                | ----- | Cyclonic Storm   |
| DAGO              | ----- | Dagoretti Corner   |
| D <sub>LTMS</sub> | ----- | Percentage deviation of MAM rainfall                       |
| EA                | ----- | East Africa  |
| EALLJ             | ----- | East Africa low- level Jet stream                          |
| ENSO              | ----- | El Niño Southern Oscillation                               |
| EOFs              | ----- | Empirical orthogonal functions                             |
| DJF               | ----- | December January February                                  |
| FAO               | ----- | Food and Agriculture Organization                          |
| GDP               | ----- | Gross Domestic Product                                     |
| Ha                | ----- | Alternative Hypothesis                                     |
| Ho                | ----- | Null Hypothesis  |
| IBTrACS           | ----- | International Best Track Archive for Climate Stewardship   |
| IOD               | ----- | Indian Ocean Dipole  |
| IPCC              | ----- | Intergovernmental Panel on Climate Change                  |

ITCZ----- Inter-Tropical Convergence Zone

JJA-----June, July, August

JTWC-----Joint Typhoon Warning Center

K-----Kelvin

KBS-----Kenya Bureau of Statistics

KMD-----Kenya Meteorological Department

LAB-----Laikipia Airbase

LLT-----Lower limit term

MAM-----March April May

MIA-----Moi International Airport

MJO-----Madden Julian Oscillation

M<sub>LTM</sub>----- MAM long term mean

MPI-----Maximum Potential Intensities

M<sub>S</sub>-----MAM rainfall of specific season

NCDC-----National Climate Disaster Center

NE-----North East

NH-----Northern hemisphere

NOAA-----North Oceanic and Atmospheric Administration

OLR-----Outgoing Longwave Radiation

OND-----October November December

PCA-----Principal Component Analysis  
QBO-----Quasi-Biannual Oscillation  
RMSE-----Root mean square error  
SE-----South East  
SEI-----Stockholm Environmental Institute  
SH-----Southern hemisphere  
SST-----Sea Surface Temperature  
SWIO-----Southwestern Indian Ocean  
TCs-----Tropical Cyclones  
ULT-----Upper limit term  
VSCS-----Very Severe Cyclonic Storm  
WMO-----World Meteorological Organization

## LIST OF SYMBOLS

|            |  |
|------------|--|
| $Z_t$      | Normalized value                       |
| $X_t$      | Variable X                             |
| $\bar{X}$  | Mean of the variable                   |
| $\sigma$   | Standard deviation of the variable     |
| $\mu$      | Mean of the sample                     |
| $\sigma_x$ | Standard deviation of MAM              |
| $\sigma_y$ | Standard deviation of Tropical cyclone |
| $E^2$      | Mean error square                      |

## CHAPTER ONE: INTRODUCTION

### 1.0 Background

Tropical cyclones are highly destructive meteorological phenomena that result in extensive damage to property and frequently lead to the loss of life in tropical regions worldwide, including Africa. Tropical cyclones are meteorological phenomena that stand out for their quick rotation, closed low-level air circulation with low pressure, strong winds, and a spiral pattern of thunderclouds accompanied by heavy precipitation ( *ReliefWeb*, 2023). In March 2019, Cyclone Idai struck Southeast Africa, causing catastrophic damage. Mozambique experienced a death toll of 670 individuals, with over 2 million people affected by the storm waters, and an estimated property loss cost of approximately 1.4 billion US dollars. Indian Ocean cyclones also have a significant influence on the climate of many East African countries, in addition to the aforementioned affects in areas directly affected by their arrival (Nhamo and Chikodzi, 2021).

Tropical cyclone (TC)-induced precipitation contributes to global precipitation. TC datasets and daily precipitation data from more than eighteen thousand rain gauges worldwide with at least more than twenty (20) years of data between 1970 and 2014 show that tropical cyclone-induced precipitation totals occur in the East Asia (more than 400 mm per year), northeastern Australia (more than 200 mm per year), while the southeastern US and the Gulf of Mexico receive between 100 and 150 mm per year. In Mexico, California, northern Philippines, northern Australia, and southern China, tropical cyclones are responsible for at least 35% of annual precipitation (Khouakhi *et al.*, 2017). Tropical cyclones have a significant impact on around 40% to 50% of the precipitation on the western coast of Australia and the southern Indian Ocean islands during the summer season. The regions of Southeast Asia and Mexico experience the impact of climatic changes over the period of the northern summer and fall. The regions of East Asia, Australia, North America, and Central America see the highest levels of precipitation caused by tropical cyclones, with the amount of rainfall diminishing gradually as you move further inland from the coast (Khouakhi *et al.*, 2017; Villarini and Denniston, 2015). The Southwest Pacific Ocean basin, the North Atlantic Ocean basin, the Northeast Pacific Ocean basin, the Northwest Pacific Ocean basin, and the Southeast Indian Ocean basin comprise the seven cyclone basins of the globe (Li *et al.*, 2019). These basins document a range of eighty to ninety tropical cyclones annually. The activity of tropical cyclone basins exhibits significant variation, with the Northwest Pacific basin



demonstrating the highest level of activity, constituting an estimated thirty percent (30%) of the overall cyclone occurrence. Cyclone activity is least frequent in the North Indian Basin, which merely explains its approximate six percent (6%) share (Cervený *et al.*, 2017).

East African countries are impacted by severe occurrences like floods and droughts caused by tropical storms in the southwest Indian Ocean. Gaining insight into the impacts of tropical cyclones in specific geographical locations can enhance the effectiveness of managing and mitigating floods and droughts. The effects of tropical storms Idai and Kenneth on the reduced rainfall during the March-April-May season, resulting in the delayed start of the 2019 seasonal rains, offer a summary of the cyclones' impact on MAM's seasonal precipitation. East African countries are linked to the disturbance of rainfall in the trajectory of moisture flow. The presence of tropical storms Idai and Kenneth in 2019 over the channel between Mozambique and northern Madagascar, accompanied by easterly wind flow across northern Tanzania, Kenya, and Uganda, led to a decrease in moisture levels in areas where the usual intake of moisture was disrupted. The geographical position and frequency of tropical cyclones in the southwest Indian Ocean impact the amount of rainfall in East Africa, as they dictate the anticipated meteorological phenomena in a specific area. These sources offer valuable insights into the factors influencing the climate in East Africa, hence enhancing the precision of weather predictions (Kebacho, 2022).

The cyclones Idai and Kenneth in 2019 had a direct impact on the amount of rainfall in Mozambique and Tanzania. This resulted in significant implications when the cyclones reached land. Moreover, they had an indirect impact on the onset of the rainy season in eastern equatorial African nations like Kenya, resulting in a delayed start to the season. The country was struck by Cyclone Idai in March 2019, which occurred simultaneously with a delayed start to the season and a meagre amount of rainfall during the MAM season. Tropical cyclones contribute to the effects by virtue of the westerly equatorial winds generated in eastern Madagascar, which in turn lead to increased rainfall. While cyclones in the Mozambique Channel do not align with westerly winds in the Equatorial Zone, they do have an effect on rainfall in East Africa. From 1980 to 2000, tropical cyclones in the southern Indian Ocean caused variations in the timing of continuous rainfall in East Africa. The reduction can be attributed to alterations in macroscopic patterns of ocean surface temperatures and atmospheric pressure (Mühr, 2019). Tropical cyclones and depressions in the Southwest Indian Ocean (SWIO) have an indirect impact on the weather and

climate of Ethiopia. The association between Ethiopia's seasonal rainfall variability and the occurrence of tropical cyclones was demonstrated using tropical cyclone correlation and composite analysis. In Ethiopia, the prevalence of drought is linked to a frequent presence of tropical storms in the Southwest Indian Ocean, whereas years with heavy rainfall experience a low number of tropical cyclones. The March-April-May season in Kenya is similarly impacted throughout these periods (Shanko and Camberlin, 1998).

### **1.1 Statement of Problem**

Tropical cyclones are severe natural occurrences that can have direct or indirect effects on regions depending on whether they are in your path or not. Storm surge, widespread flooding that ruins infrastructure, high winds that destroy structures, heavy torrential rain, and economic losses are all direct consequences of tropical cyclones (Kunze, 2021; Lenzen *et al.*, 2018). The primary concern is to enhance the predictive capabilities for the extended rainy season by investigating the correlation between the incidence of tropical cyclones and the March-April-May season, since this would enhance the mechanisms that lead to precipitation. There is a lack of research evaluating the effects of tropical storms that occur in the Southwest Indian Ocean (SWIO) during Kenya's prolonged rainy season (March–April–May).

### **1.2 Research Questions**

- 1) What is the current temporal and spatial distribution of MAM seasonal rainfall in Kenya?
- 2) How is the temporal distribution of tropical cyclones over SWIO?
- 3) Does the frequency of tropical storms in the Southwestern Indian Ocean region have an effect on the MAM seasonal rainfall in Kenya?

### **1.3 Objectives**

The study's primary goal was to look into the relationship between the frequency of tropical cyclones in the southern Indian Ocean and Kenya's rainfall totals from March to May.

In order to do this, the following precise goals were pursued:

- (i) To define Kenya's present rainfall patterns in terms of both space and time for the months of March, April, and May

- (ii) To determine the intra-seasonal variability and tendencies the of frequency occurrence of tropical cyclones North of 20°S and West of 60°E in the Southwestern Indian Ocean from November-1979 to April-2019
- (iii) To examine the potential link between tropical cyclone frequency in the SWIO and rainfall variability during the MAM seasonal rainfall in Kenya

#### **1.4 Justification**

Tropical cyclones (TCs) are meteorological phenomena that form in oceanic regions and have the potential to create catastrophic catastrophes in a variety of tropical locations, including the southwestern Indian Ocean (SWIO) region along Africa's coastline. In February and March 2023, Tropical Cyclone (TC) Freddy pounded South Africa and the Indian Ocean, wreaking havoc in Mozambique, Malawi, and adjacent countries (*Southern Africa*, 2023). The tropical cyclone in the Southwest Indian Ocean (SWIO) region is causing significant damage to infrastructure, resulting in loss of life and displacement of people due to floods caused by intense and prolonged rainfall. Additionally, it is also leading to a decline in economic development activities. A study was done to investigate the behavior and impacts of tropical cyclone Idai, which had a substantial impact on a large area of the Southwest Indian Ocean (SWIO) region from March 4th to 21st, 2019. Tropical cyclone Idai caused a significant increase in atmospheric conditions, particularly in the southern region of Africa and the neighboring areas of Mozambique. This phenomenon also affected the weather in specific places located around the equator and the southern section at a latitude of 12°S. More precisely, the regions that were impacted experienced minimal differences in wind speed and direction at different altitudes, with values ranging from -3 to 3 m/s, at the exact spots where the cyclone hit land. Conversely, more powerful wind shear values ranging from 10 to 40 m/s were detected in the northern and southern regions of the Mozambican channel. The tremendous wind speeds and torrential precipitation of tropical storm Idai caused significant devastation. The cyclone resulted in fatalities and inflicted significant harm on infrastructure and residential buildings in Mozambique, Malawi, and Zimbabwe. The cyclone resulted in an approximate financial loss of \$2.2 billion. Tropical cyclone Idai resulted in a substantial elevation in moisture levels, varying from 80% to 90% in the low-lying areas of Mozambique. The Idai storm disturbed the regular patterns of rainfall in northern Kenya and Tanzania, exacerbating the severe food shortage in northwestern Kenya, namely in Turkana. The typhoon Idai led to extensive flooding,

which had a profound effect on various socioeconomic activities, resulting in substantial human casualties, injuries, financial losses, and infrastructure damage. Residents in eastern Mozambique were compelled to evacuate their residences for an extended period of time as a result of the likely occurrence of waterborne illnesses such as malaria and cholera (Kai *et al.*, 2021).

## **1.5 Area of study**

The location and climate of the study region are discussed.

### **1.5.1 Location**

Kenya is situated between 34° E and 42° E longitudes, and between 5° S and 5.5° N latitude. It is located in the African continent's eastern region. The area under investigation features a 500-kilometer coastline that borders the Indian Ocean, as Figure 1-1 illustrates. Kenya has a diverse topography, with low-lying areas, highlands, and the Great Rift Valley, which stretches from the northwest to the southeast of the nation. Moreover, the area has other amazing geographical features, like Mount Kenya, the second-tallest mountain in Africa and a dormant volcano. The country in question is located adjacent to Ethiopia and South Sudan to the north, Somalia to the east, Tanzania to the south, and Uganda to the west. The country has a border that stretches for 3,446 kilometers and covers an area of 580,728 square kilometers. The region consists of 98 percent land and 2 percent water. The peak of Mt. Kenya is the highest point in its geographical region, with an elevation of at least 5197 meters above sea level (Ingham *et al.*, 2023).

Arid and semi-arid lands (ASAL) account for roughly 85 percent of Kenya's total land area of 580,728 Km<sup>2</sup>. Kenya's current population, however, exceeds 47.6 million people, with 30 percent residing in the ASAL region (Kenya National Bureau of Statistics, 2019; Nicholson, 2017).

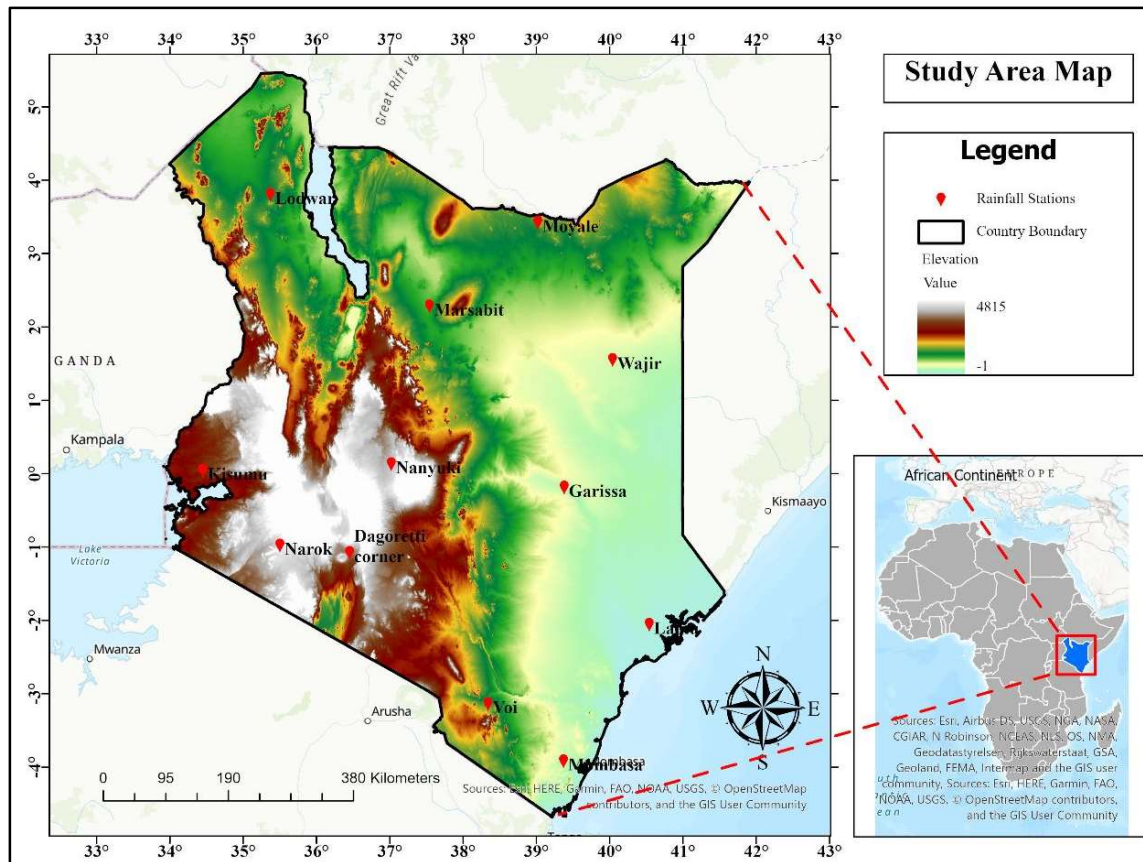


Figure 1-1: Map of area of study showing the topographic elevation (m), and the representative rainfall stations and its location in Africa

(Source: The map was developed by the author in ArcGIS software, May 2023)

### 1.5.2 Weather and Climate of Kenya

Kenya has two distinct rainy seasons, which are indicative of a bimodal rainfall pattern. March through May is when the first phase, referred to as the long rains, occurs. The second phase, which is known as the short rains, lasts from October through December. These seasons are impacted by the Intertropical Convergence Zone's (ITCZ) migration between the Northern and Southern hemispheres. The system induces a short period of precipitation as it progresses in the southern direction (Gitau *et al.*, 2013). However, the intensity, magnitude and timing of these rains vary greatly throughout the year, in space and time. Rainfall varies from more than 2,000 mm per year in some locations to less than 300 mm per year in northern Kenya. Drought and floods are the most common climate risks in Kenya, with widespread drought affecting at least 23 million people. Similarly, El Niño has a substantial impact on Kenya's climate, increasing precipitation and causing floods (Kijne *et al.*, 2009). The seasonal climate of East Africa (Kenya, Tanzania, and

Uganda) is influenced by synoptic-scale pressure systems in the western Indian Ocean and adjacent landmasses. (Zinke *et al.*, 2009). Predominantly, the wind regimes between December and March comprise winds from the northeast in the northern part of the equator and from the southeast in the southeast part of the equator. December-January-February (DJF) is typically dry, with only a few instances of precipitation due to the microclimate. From March to May, the rainy season lasts, with winds moving from east to west in both hemispheres. The June-July-August (JJA) season hardly rains in eastern Kenya as the winds during this season are mainly from the south, while the southern part of Kenya has southeasterly winds, but the west receives rain from winds. west of the Congo region (Koech, 2014, Slingo *et al.*, 2005). More than two-thirds of Kenya receives less than 500 millimeters of rain annually. Precipitation variability is more prevalent in desert and semi-arid environments. The period from mid-December to mid-March is characterized by hot and arid weather, whilst June to August often have cool and dry conditions, however certain areas in western Kenya may have a third rainy season.

The Arid and Semi-Arid Lands (ASAL) include over 80% of Kenya's territory and support 70% of its livestock population, as well as around 90% of its wildlife. The yearly precipitation ranges from 150 mm to 550 mm, with the Semi-Arid zone receiving the highest amount of rainfall. The ASAL region is characterized by persistent harsh weather conditions, including high temperatures and evapotranspiration, which occur consistently throughout the year (Grove *et al.*, 1977). These regions typically experience scorching or occasionally exceptionally high temperatures throughout the summer, and mild or chilly winters with limited precipitation. Hot semi-arid climates are predominantly located on the periphery of subtropical deserts, many of which are situated in Africa.

### **1.5.3 Systems Influencing Rainfall over Kenya**

These are systems that influence weather patterns which are significant characteristics, specific in regional effects, and a definite behavior in oscillation, and normally used as indices to monitor how a given weather pattern may be affect a given region (Thornton *et al.*, 2014). They may not necessarily originate in their areas of impact but may be far away. The weather fluctuations in East Africa are caused by various phenomena, including El Nino/Southern Oscillation (ENSO), Indian Ocean Dipole (IOD) Mode, Quasi-Biennial Oscillations (QBO), and Madden Julian Oscillation (MJO).

### 1.5.3.1 Inter-Tropical Convergence Zone

The Intertropical Convergence Zone (ITCZ) is a narrow band of low barometric pressure that encircles the Earth's equator and is caused by the convergence of air masses from the Southern and Northern Hemispheres. The current weather pattern is distinguished by high levels of atmospheric moisture, significant precipitation events, dense cloud cover, and intermittent gentle winds. The orographic orientation in Kenya is determined by two distinct arms, the southern arm and the zonal arm. A meridional arm component is formed at this location by the convergence of westward winds from the Atlantic Ocean and eastward winds from the Indian Ocean. Rainfall is delivered to the regions it passes through by the zonal component of the Intertropical Convergence Zone, which exhibits regular oscillations in a north-south orientation. The existence of two discrete rainfall periods, referred to as the long and short rainy seasons, is linked to the movement of Kenya's Inter-Tropical Convergence Zone. East Africa is home to a large synoptic system that has a major impact on the seasonal distribution of rainfall (Asnani and Kinuthia, 1979). The north-south migration of the sun, which happens in both hemispheres, significantly affects the seasonal rainfall patterns in East Africa. The disturbance of the Intertropical Convergence Zone has a substantial impact on the initiation of convection in the designated geographic area. As a result of the Intertropical Convergence Zone's migration between hemispheres, East African precipitation patterns are affected. The completion of this undertaking is significantly obstructed by the impact of wind patterns, seasonal cycle fluctuations, large-scale teleconnections, and the unpredictability inherent in spatial patterns (Nicholson, 2017). The wide range of seasonal rainfall frequencies in the EA is due to strong effects from convergence in the lower troposphere. Likewise, surface divergence predominates, whereas convergence is advantageous during moist seasons and results from topographic and littoral uplift in the western highlands. Seasonal variations in precipitation impact the seasonal rainfall pattern in East Africa. The uplift in the western highlands and coastal region during the monsoon season is mostly caused by positive integrated regional convergence in the lower troposphere, making it a key factor. The primary attribute of this elevation is the dispersion of the surface (Yang *et al.*, 2015). The East Africa's seasonal rainfall cycle has been impacted by a combination of rising precipitation levels and reduced tropospheric divergence (Nicholson, 2017). Interregional convergence, on the other hand, is favorable during the wet season. The low pressure zone is the typical location for intense precipitation. The transfer of heat and energy from the Atlantic Ocean to the northern hemisphere through the equatorial region is responsible for the

ability of this zone to produce rainfall. Schneider *et al.* (2014), the intertropical convergence zone migrates to a warmer hemisphere on average over an extended season, with El Nino episodes functioning as exceptions. Furthermore, three to four weeks' elapse between the system's activation and the sun's latitudinal shift. Mesoscale circulation is aided by inland lakes and different topographical features throughout the area. The irregularity in the intertropical convergence zone course can be traced to the Northern Hemisphere's greater land mass, which leads it to migrate more quickly southward than northward. As a result, the northward march experiences more precipitation (Schneider *et al.*, 2014).

### 1.5.3.2 El Nino Southern Oscillation

Researchers from several countries have utilized comprehensive statistical analysis and advanced technological tools to develop a comprehensive climatology of worldwide precipitation patterns. This has been achieved by the computation of anomalies and the integration of satellite observations with measured precipitation data. Changes in the monsoon systems' patterns have been noted in the Pacific, Indian, and Atlantic Oceans. The interplay between mid-latitude westerlies and other meteorological systems resulted in variations from typical precipitation patterns in both tropical and extra-tropical locations (Dai and Wigley, 2000).

The presence of the El Niño-Southern Oscillation (ENSO) phenomenon is the main factor responsible for drought occurrences in Kenya. This climate system has a substantial influence on both the short and long rainy seasons in East Africa. More precisely, the beneficial impacts of El Niño Southern Oscillation are more evident throughout the October to December (OND) timeframe. Between 1997 and 2016, there was a significant incidence of this phenomena, especially when El Nino events occurred, followed by the emergence of La Nina the following year, as seen in 1999/2000 and 2017 (Kijazi and Reason, 2005; Uhe *et al.*, 2018; Zhang *et al.*, 2021).

### 1.5.3.3 Madden Julian Oscillation

A circulation wave that moves eastward and completes a circle around the Earth characterizes the Madden Julian Oscillation (MJO), an atmospheric phenomenon that happens in tropical regions (Madden and Jullian, 1971, 1972). The object under investigation has an observed life expectancy of thirty to sixty days, and its speed is measured at five meters per second. The phenomenon



exhibits observable characteristics concerning temperature variations, pressure anomalies, and zonal winds. The Madden-Julian Oscillation is responsible for the observed variations in intra-seasonal precipitation variability in Kenya between March and May and October and December (Pohl and Camberlin, 2006). The Madden-Julian Oscillation exerts a substantial influence on the fluctuation of precipitation during the March-April-May season. It accomplishes this by promoting the occurrence of premature and intense rainy episodes at an earlier stage of the season. Conversely, when there is a strong Madden-Julian Oscillation signal during October-November-December, it is linked to prolonged periods of dry weather throughout the coastline region of East Africa. Nevertheless, this phenomenon exhibits annual variations.

Omeny *et al.*, (2008), demonstrated that the Madden-Julian Oscillation may be effectively used to accurately predict the fluctuations within a season in the western part of East Africa (EA). The correlation between Phases 3 and 4 of the Madden-Julian Oscillation and moisture transport in East Africa can be attributed to the dominant displacement of the Congo air mass, which consistently results in increased moisture content. The presence of arid conditions is strongly associated with the easterly flow, which is a climatological phenomenon. This particular climatic system has a significant impact on controlling the larger climate patterns found in East Africa (Finney *et al.*, 2020).

#### 1.5.3.4 Quasi Biannual Oscillation

The Quasi Biannual Oscillation (QBO) is a recurring pattern of equatorial zonal winds at 30 millibars in the lower tropical stratosphere. This cycle repeats approximately every 22–28 months. The wind regime undergoes a gradual descent of 1 kilometre every month from the lower stratosphere until it reaches the tropopause. Easterlies and westerlies have different downward propagation patterns. However, the amplitude of the easterly phase is twice as large as that of the westerly phase (Baldwin *et al.*, 2001). Previous research discovered a link between East African rainfall and quasi-biennial oscillations. Lower stratospheric flow is associated with increased easterly rainfall and decreased westerly rains (Ng'ongolo and Smyshlyaev, 2010). Previous studies have established a correlation between lower stratospheric zonal patterns and seasonal precipitation, whereby the easterly phase has a positive relationship with increased rainfall, while the westerly phase demonstrates a negative association with precipitation levels. A strong positive correlation was seen between rainfall in East Africa, lower zonal winds in the equatorial

stratosphere, and the MAM season. This suggests a linear relationship where changes in one variable can be used to forecast changes in the other variables (with a non-zero logarithmic link). The link was especially noticeable in the western region (Ash & Matyas, 2012; Indeje *et al.*, 2000; Vellinga & Milton, 2018).

#### 1.5.3.5 Indian Ocean Dipole mode

The Indian Ocean Dipole Mode is distinguished by a dynamic and variable pattern of sea surface temperatures (SSTs) in the Indian Ocean, characterized by nonstationary behavior and alternating oscillation. The contrasting abnormalities in sea surface temperatures found in the Western and Eastern Tropical Indian Oceans cause the Indian Ocean Dipole to occur in positive and negative phases (Samrin *et al.*, 2019). It is linked to significant year-to-year variations in ocean-atmosphere conditions across the Indian Ocean's equatorial region.

Hameed, (2018), the Indian Ocean dipole has its greatest variability during the summer and fall seasons, with a notable peak coming near the end of October. Prior research has demonstrated that the Indian Ocean dipole is a distinct phenomenon that has a substantial impact on climatic patterns in the East African region, even though it was initially linked to the El Niño-Southern Oscillation. The Indian Ocean dipole impacts climate variability by causing extreme weather events in East Africa during its positive and negative phases (Ash and Matyas, 2012; Marchant *et al.*, 2007). The years 1982, 1983, 1994, 1997, 2006, 2012, 2015, and 2019 were the ones that had positive readings for the IOD (Ratna *et al.*, 2021) .

#### 1.5.3.6 Subtropical Anticyclone

Synoptic anticyclones are usually semi-permanent high-pressure cells that determine wind flow based on which hemisphere has high pressure. The characteristics of the wind passing over the region will be determined by the origin of the wind (Tyson *et al.*, 1996). From the 1950s to around 2010, the SSTs warming during MAM season in the Pacific Ocean (Ondiko and Karanja, 2021) especially around the tropics led to significant changes in rainfall across Eastern Africa (Slingo *et al.*, 2005). Warming of the west Pacific SSTs lowers atmospheric flow by decreasing the Somali Jetstream. It influences the influx of moisture from the ocean across Eastern Africa (Hoell and Funk, 2013).

The Azores high-pressure system and the Arabian ridge in the northern hemisphere, as well as the St. Helena and Mascarene highs in the southern hemisphere, all have a significant impact on African weather patterns. Seasonal temperature swings are caused by the periodic intensification of high-pressure systems in winter, followed by their attenuation in summer. Temperatures vary significantly between the winter and summer seasons. Wind motion is primarily propelled by pressure differentials caused by unequal thermal energy distribution, resulting in the movement of air from higher-pressure regions to lower-pressure regions. The pressure differential at a particular location causes the formation of various wind patterns with variable characteristics (Behera and Yamagata, 2001).

## CHAPTER TWO: LITERATURE REVIEW

### 2.0 Introduction

This section provides an overview of rainfall variability, climate systems, and fluctuation mechanisms in different geographical regions, including the specific research topic.

### 2.1 Rainfall Variability

An increase in precipitation and a fluctuating hydroclimate, characterized by variations in both wet and dry extremes, will affect approximately 66% of the Earth's land area. The rise in precipitation variability is most noticeable in areas with a consistent high level of moisture, where the percentage increase in variability exceeds the percentage increase in average precipitation (Konapala *et al.*, 2020; Dong *et al.*, 2018). Li and Li (2019), moisture availability can cause uniformly higher precipitation variability. These are linked to thermodynamics processes in the atmosphere. Precipitation variability changes are extremely location-dependent due to negative dynamic impacts associated with decreased circulation variability. The heightened fluctuation in rainfall patterns presents a fresh obstacle to infrastructure and significantly impacts the year-to-year variation in climate resilience of human society. Between the mid-1980s and 2010, long rains became less wet, with a decrease of -0.65 to -2.95 mm per season per year. However, since the mid-1980s, there has been a trend of long rains becoming wetter, with an increase of 1.44 to 2.36 mm per season per year. These patterns, combined with significant fluctuations from year to year, have an impact on the intensity and frequency of severe floods and droughts, the resilience of food and energy systems, vulnerability to water- and vector-borne diseases, and the stability of ecosystems (Palmer *et al.*, 2023)

The current model of two rainy seasons caused by the biannual movement of the Intertropical Convergence Zone across the equator is insufficient. The Long rains should not be regarded as a singular season due to its distinct characteristics, causes, and relationships that vary considerably from month to month. The frequency of continuous rainfall has gradually declined in the past few decades. The Madden-Julian Oscillation (MJO) now significantly influences both year-to-year and within-season fluctuations. The intensity of the anomalies in the Pacific and Indian Oceans, on the other hand, is critical in determining the trend's direction. Droughts have become more severe in duration and severity, and they frequently persist even during the rainy season. The underlying causes of these droughts are poorly understood. When compared to traditional forecast models that

focus on factors such as sea surface temperatures and the El Niño-Southern Oscillation, atmospheric variables provide greater dependability in seasonal forecasts (Nicholson, 2017).

While researching circulation patterns connected with MAM rainfall in Kenya, Ayugi *et al.*, (2018) observed a decrease in rain which has created a concern to agricultural institutions around. Statistical evaluation of trends has revealed the trends in the MAM rainfall are decreasing. Considerable rainfall amounts are usually caused by low-level surface convergence and upper-level atmospheric divergence that is aided by the advection from well-positioned anticyclones in the Indian Ocean.

On the contrary, dry conditions are caused by inverse Walker circulation conditions. Positive SST anomalies and negative anomalies of outgoing longwave radiation (OLR) influence MAM rainfall during this period (Schwarzwald *et al.*, 2022). Kenya's rainfall temporal distribution demonstrates how erratic the weather can be both in space and time. Ayugi *et al.*, (2018), shows that temporal rainfall variability from 1971 to 2010 has the highest rainfall in 1997 of 1309 mm and the lowest 2000 of 609 mm. The highest of rainfall ever in the 34 station was 3673 mm in Kisii station and lowest in Lodwar station with 54.2 mm annually. This study also showed that there is a decrease in MAM seasonal rainfall in Kenya.

The variable weather in Kenya has led to extreme rainfall events occurrence which has mostly affected heavily the Arid and Semi-Arid lands. Between 1980 to 2019, there has been over five events of drought recorded (1983/84, 1992, 1995/96, 1999/00, 2004/06) affecting millions of people and loss of livestock (Ondiko and Karanja, 2021).

## **2.2 Effects of Tropical Cyclones on rainfall**

A tropical storm can have either direct or indirect effects on your location, depending on whether you are directly in its path. Most places in the world have seen rain as a result of tropical cyclones. Tropical cyclone-induced rainfall is highest in Eastern Asia (above 400 mm per year), followed by northern Australia (above 200 mm), northeastern America (between 100 and 150 mm per year), and the Gulf of Mexico coast. Tropical cyclones cause 35–50% of rainfall in northern Australia, southeast China, the northern Philippines, and Mexico. Tropical cyclone-induced rainfall accounts for 40–50% of the rain that falls on Australia's west coast and on islands south of the Indian Ocean

during the summer months in the southern hemisphere (Khouakhi *et al.*, 2017; Kubota and Wang, 2009).

There has been a decline in global tropical cyclone patterns, including both the frequency of cyclones and the total energy they generate. The reduction is attributed to diminishing trends in the Northwestern Pacific. Hurricane storms with a short duration and rapid strengthening, reaching wind speeds of above 50 knots per day, have become more common worldwide, causing devastation associated with tropical cyclone. The increased potential intensity of tropical cyclones is attributed to the technicalities of their development stage. Damages have increased as coastal assets have increased in value. The constant presence of La Nia-like conditions from 1990 to 2021 can be attributed to the decline in storm frequency and global accumulated cyclone energy (ACE). These conditions favor the formation of tropical cyclones, particularly in the North Atlantic, while reducing the occurrence of tropical cyclones in the North and South Pacific. Regional and global climatic shifts can be attributed to global warming and changes in the El Nino Southern Oscillation pattern (Klotzbach *et al.*, 2022).

The increased frequency of tropical cyclones making landfall in the Southwest Indian Ocean over the last six decades, as shown by trajectory data spanning 60 to 160 years, can be attributed to improved record quality. There is insufficient statistical evidence to support the changing patterns and oscillations in the number of cyclones, which are influenced by atmospheric forcing processes such as the El Nino Southern Oscillation and the Quasi Biennial Oscillation. The fluctuations in Madagascar's southern region can be attributed to the southerly movement of the isotherm by 26 degrees and the reduced control of the airflow during the La Nina phenomenon. The observed trends do not indicate the presence of significant storms, but rather the utilization of sophisticated technical methods for detecting and storing storm-related data (Fitchett and Grab, 2014).

Because most cyclone basins lack sufficient monitoring equipment, measuring natural anomalies in global tropical cyclone activity is difficult, according to Henderson-Seller *et al.*, (1998). The data for the North Atlantic and western North Pacific basins are robust, exhibiting substantial multi-decadal fluctuations, particularly in relation to devastating hurricanes in the Atlantic. However, there is no compelling evidence of enduring patterns over the long period. The latest thermodynamic assessment of maximum potential intensity (MPI) for tropical cyclones aligns

closely with empirical evidence. Despite some uncertainties associated with these MPI approaches, such as their susceptibility to parameter variations and the exclusion of certain potentially important interactions caused by ocean splashes, the upper ocean thermal structure and behavior of the eye and eyewall can be used to forecast the current and future maximum intensities of tropical cyclones. These predictors are reliable and accurate at forecasting the intensity of tropical cyclones. As a result, they can be used to issue timely warnings of severe storms and inform people about their potential consequences. According to recent studies, the cyclone MPI will remain unchanged or grow by 10–20%. The projected changes are minor compared to the reported normal variations as they fit within the margin of error in current investigations. The projected intensity could be minimal by excluding ocean dew, momentum limitation, and possible fluctuations in the acceleration rate of 300 hPa (Henderson-Sellers *et al.*, 1998).

Most regions of the world receive variable amounts of precipitation over land that's relative to the amount of warming. This has been revealed by most climate models, in which 66% of land demonstrates robust increased rainfall variability in the seasonal means. Precipitation variability increases by 3–4 percent per Kelvin (K) globally, by 4-5 percent per Kelvin over land, and by 2-4 percent per Kelvin over the ocean, and is astonishingly robust across timescales ranging from daily to decadal. Most often, geographies, periods, and models increase precipitation variability more than mean precipitation (Pendergrass *et al.*, 2017).

Tropical cyclones are oceanic system that influence weather activities in the atmosphere. This makes it vital to comprehend their behavior and impact on rainfall patterns in temporal and spatial distribution. According to Lima *et al.*, (2021), Tropical cyclones are more prevalent in the Northeastern Atlantic Ocean Basin. Recent study indicates a rise in both the frequency and strength of Tropical cyclones. Scientists conducted a study in the northern Indian Ocean to analyse the effects on the Bay of Bengal area.

Storm behavior across Northern Atlantic is related to sea surface temperature, which was caused by global rise in mean temperature. Goldenberg *et al.*, (2001)) found that, The Bay of Bengal in the northern Indian Ocean has experienced a fivefold increase in the frequency of tropical cyclones compared to the Arabian Sea. The storm basin in question has had a higher number of catastrophic

events and fatalities caused by tropical cyclones compared to the western Indian Ocean (Sahoo and Bhaskaran, 2016).

Tropical cyclones occur more frequently in the Bay of Bengal than in the Arabian Sea, according to climate data. However, in recent years, the Arabian Sea has seen more tropical cyclones than the Bay of Bengal. There has been a significant increase in the strength, frequency, and duration of cyclonic storms and very severe storms in the Arabian Sea from 1982 to 2019. In particular, the frequency of severe cyclones in the Arabian Sea has increased by 52% between 2001 and 2019. In contrast, there has been an 8% decrease in the Bay of Bengal. In the Arabian Sea region, the duration of cyclonic storms has increased by 80%, and the occurrence of Very Severe Cyclonic Storms is about three times higher in the recent period compared to the years between 1982 and 2000 (Deshpande *et al.*, 2021).

Wing *et al.*, (2007), showed that as global sea surface temperatures rise, tropical storm frequency and intensity will be impacted by climate change. It causes water to build up energy, which in turn causes cyclones. In the northern Atlantic basin, tropical storm intensity has increased since the 1970s ( Grossmann and Morgan, 2011; Kossin *et al.*, 2007; Wang and Wu, 2012). Tropical storm basins have exhibited a discernible rise in the intensity of tropical cyclones, while the southwestern North Pacific, South Pacific, and eastern South Indian Ocean have experienced a decline. Wing *et al.*, (2007) found that a higher frequency of tropical cyclones enhances the likelihood of rainfall-producing systems.

According to Mendelsohn *et al.*, (2012), one potential consequence of greenhouse gas emissions is an increase in extreme damage. They quantified how climate change affects tropical storm since future income losses increases will almost triple the damage from Tropical cyclones even if climate change does not occur. Climate change is projected to amplify the occurrence of high-intensity ocean storms in certain basins. Tropical cyclone damage resulting from climate change is observed in North America, East Asia, the Caribbean, and Central America.

From research by Samrin *et al.*, (2019), shows that even though Indonesia is a cyclone-free zone but is affected by nearby cyclones with tropical cyclone rainfall causing flooding; consequently, monitoring its growth, intensity, and movement is crucial. Cyclone Cempaka which was reported



in November 2017 and lasted three days, generated increased precipitation over Indonesia's Java Island.

Tropical Cyclone Eline caused devastating floods in Southern African countries in February and March 2000, causing major property damage and loss of life. It had a widespread influence across southern Africa, with heavy rainfall falling in the drylands of Southern Namibia during this period. Cyclone Eline developed over the Southwestern Indian Ocean but affected nearly the entire region from east to west, helping drier with enhanced rains but damaging the eastern coast, where it made landfall (Reason and Keibel, 2004). The study highlighted how vital it is to investigate the linkage of a tropical cyclone over the southwestern Indian Ocean to Kenya. Even though we are not in the cyclone genesis region, the probability of indirectly affecting rainfall by tropical cyclones over SWIO are high. This has been shown to have an effect on the Ethiopian rainy season, creating dryness (drought) whenever there is a high occurrence of cyclones over the SWIO (Shanko and Camberlin, 1998), while in some regions it indirectly increases precipitation, as occurred during the Baiu Season, 1999, in Kyushu, Japan. The intense rain was caused by Typhoon Maggie, 2,000 kilometers away (Samrin *et al.*, 2019; Yoshida and Itoh, 2012)

Finney *et al.*, (2020) demonstrate that tropical cyclone formations over east Madagascar are linked to MJO phases 3 and 4. Similarly, these MJO phases correspond to times when there is a westerly flow of air mass from the Congo region, bringing wet conditions to east Africa. When the flow reverts to easterlies, dry conditions prevail in eastern Africa, contributing to rainfall variability over the long season. The study by MacLeod *et al.*, (2021) in western Kenya suggests that heavy rainfall episodes are a teleconnection of MJO presence in the equatorial East African region. Koech, (2014) observed that cyclones over the southern Indian Ocean lowered rainfall by up to 90% in some regions. He also examined the elements contributing to wet spells during the dry December–February season. Dry periods during the OND season were related to cyclone occurrence across the ocean.

Many studies have been done on the possible causes of rainfall variability in Kenya but no or little work has done to related the cyclone occurrence over the southwestern Indian ocean with its rainfall variability during long rain season in Kenya.



Table 3-1: Tabular display of Synoptic Rainfall Stations with Latitude, Longitude, Elevation, and Long Term Mean of MAM Seasonal Rainfall over the research region.

| Station   | Latitude (°) | Longitude (°) | Elevation(m) | Long Term Mean MAM (mm) |
|-----------|--------------|---------------|--------------|-------------------------|
| Lodwar    | 3° 42' N     | 35° 22' 12"   | 506          | 95.7                    |
| Moyale    | 3° 33' N     | 39°01' 48"    | 1097         | 367.1                   |
| Wajir     | 1° 27' N     | 40°02' 24"    | 244          | 140.4                   |
| Garissa   | 0°17' 24" S  | 39°22' 48"    | 147          | 119.5                   |
| Lamu      | 2° 09' 36" S | 40° 32' 24"   | 30           | 462.7                   |
| Mombasa   | 4° 01' 12" S | 39° 22' 12"   | 55           | 414.6                   |
| Voi       | 3° 14' 24" S | 38°20' 24"    | 597          | 195                     |
| Dagoretti | 1° 10' 48" S | 36° 27' 00"   | 1798         | 491.3                   |
| Nanyuki   | 0° 01' 48" N | 37° 01' 12"   | 1905         | 218.4                   |
| Narok     | 1° 03' 36" S | 35°30' 00"    | 1890         | 315                     |
| Marsabit  | 2°10' 48" N  | 37°32' 24"    | 1345         | 361.8                   |
| Kisumu    | 0°3' 36" S   | 34°27' 00"    | 1145         | 561.3                   |

### 3.1.2 Tropical Cyclone Data

The International Best Track Archive for Climate Stewardship (IBTrACS) obtained monthly data on tropical cyclone occurrences from November 1979 to April 2019, although the other data archive centers were used for validation. Data supplied information on cyclone stages, wind speeds, location, time, and pressures. These additional centers are the Cooperative Institute for Meteorological Satellite Studies (CIMSS), National Climate Disaster Centre (NCDC), NOAA, and Joint Typhoon Warning Centre (JTWC). Cyclone records for the study covered cyclonic systems ranging from tropical storms to powerful tropical cyclones in the SWIO basin.

### 3.1.3 Data Quality Control

Data quality control was performed to remove errors or outliers that may have occurred as a result of a defective instrument, transmission to archiving centres, or human mistake when reading and processing. This was evaluated using a single mass curve displayed to depict a straight line for data with consistency, but kinked lines suggest data inconsistency, which is explored and remedied if necessary (Nyakwada *et al.*, 2009).

### 3.1.3.1 Estimation of missing data

The estimation method is used to fill in missing data in zones with more than 10% gaps in the dataset. Normal ratio, Arithmetic means, correlation analysis, regression analysis, Thiessen, and the isohyet approach are some estimation methods that can be used to fill in missing data in any climatic dataset (Mueni, 2016; Rwigi, 2014). The Normal ratio method was employed to compute data gaps by utilizing adjacent stations with complete data.

### 3.1.3.2 Normal ratio method

The Normal ratio approach was used to estimate data for the gaps in the dataset, with the goal of minimizing the percentage gap to less than 10%. It should be noted that most monthly climate data records did not have any gaps that needed to be filled before further investigation. The inclusion of missing records from a specific station was limited to those that did not exceed 10% of the overall dataset or those that had a dataset for the station totaling 90% of the total dataset (WMO, 1966). In the study's analysis, Equation 1, which represents the Normal ratio approach, was used to fill in the missing data record for MAM season rainfall and tropical cyclone data (Jamal, 2017.).

$$X_{Aj} = \frac{X_{Bj}}{X_B} \cdot \overline{X_A} \dots\dots\dots(1)$$

In equation 1,  $X_{Aj}$  is missing data for station A in year j, B is station with complete data in years j,  $\overline{X_A}$  and  $\overline{X_B}$  long-term averages for the two stations, A and B.

Data inconsistencies are represented by the kinked line on the graph, whereas consistency is symbolized by the straight line. This results in an increase in the error margin of the research paper unless the voids that are not filled in and any anomalies that are rectified.

### 3.1.3.3 Single mass curves

The cumulative climatological MAM seasonal rainfall for each homogenous zone is shown to create a single mass curve. This innovation made it easier to find data with inconsistencies in regions with sparse data, gaps, or outliers

A graph was created by plotting the cumulative rainfall data over time in order to assess the uniformity of the data. Single mass curves offer prompt insights about the data's coherence. A

linear trend in a univariate dataset indicates that the data is consistent and lacks variability. When dealing with non-homogeneous data, the ratio of the two straight lines is used. The rainfall data prior to the break are multiplied by the ratio of slopes after and before the break (Muthama *et al.*, 2008; Wakachala *et al.*, 2015).

## **3.2 METHODOLOGY**

This section offers a detailed explanation of the methodologies used to tackle the various goals of the study. This work aims to analyze two primary factors: the geographical and temporal variance in MAM seasonal rainfall in Kenya, and the frequency and trends of Tropical Cyclones occurrence. The research seeks to examine the possible correlation between the frequency of Tropical Cyclone occurrences in the Southwest Indian Ocean (SWIO) and the long-term fluctuations of MAM seasonal rainfall. The inquiry will utilize lag correlation analysis, applying the Taylor diagram and time series analysis. The interplay between synoptic-scale systems and local-scale systems, including winds, landscapes, water bodies, and radiation, leads to spatial and temporal fluctuations in the distribution of precipitation at a specific place. The presence of local circulations in mountainous regions and the occurrence of sea breezes contribute to the heightened intensity of precipitation events during periods of low-pressure gradient associated with radiation days (Granger, 1987; Knerr *et al.*, 2020).

### **3.2.1 Assessment of the Spatial and Temporal Patterns of MAM Seasonal Rainfall in Kenya**

The purpose of this study is to examine the spatial and temporal variations of MAM seasonal rainfall in Kenya using two methodologies: spatial interpolation analysis, which entailed the creation of geographic maps, and temporal analysis, which primarily focuses on time series analysis. Comprehensive information regarding these strategies is expounded upon in the subsequent sub-section. The spatial analysis encompassed the utilization of rainfall spatial plots to visually represent the distribution patterns. Time series analysis was predominantly employed to detect seasonal variations in MAM seasonal rainfall in Kenya.

### 3.2.1.1 Rainfall Anomalies

The rainfall anomalies were utilized to evaluate the fluctuations in precipitation within the region across the years. Values beyond the positive threshold (one standard deviation) were indicative of an intensified rainfall season, whilst values falling below the negative limit (lower standard deviation) were associated with a suppressed MAM (March, April, May) season. Time series analysis was employed to examine the temporal variation of MAM rainfall anomalies in Kenya from 1980 to 2019.

The datasets were standardized using Equation (2)

$$Z_t = \frac{x_t - \bar{X}}{\sigma} \dots\dots\dots (2)$$

In the Equation 2,  $Z_t$  represents the normalized values,  $\sigma$  the standard deviation,  $X_t$  is the variable, and  $\bar{X}$  the mean of the variables.

This facilitates the visualization of rainfall and tropical cyclone data on a single graph for the homogeneous zones characterized by distinct climate zoning.

### 3.2.1.2 Spatial Distribution of MAM seasonal Rainfall

The utilization of spatial maps is employed in this methodology to visually represent the spatial distribution of rainfall. The process involves the utilization of overlays to analyze the placements, characteristics, and interconnections of elements within spatial data (Borregaard *et al.*, 2008). Spatial interpolation is a method used to estimate variables at locations in geographic space where data is not available. This estimation is derived from the values recorded at other sites. Analyzed rainfall data was used to investigate the spatial variability within the research area.

Large-scale and small-scale weather systems interact to influence the distribution and timing of rainfall in a given region. These weather systems are location- and time-dependent. The diurnal fluctuation observed within synoptic regimes is caused by the daily transition between day and night. Days with elevated radiation levels and reduced air pressure can lead to the development of localized circulation patterns in mountainous areas. These circulation patterns, when combined with sea breezes, might contribute to an intensification of precipitation (Granger, 1987; Knerr *et al.*, 2020).

### 3.2.1.3 Temporal distribution of MAM seasonal Rainfall

Time series analysis helps understand data patterns that evolve over time. Time series analysis can visualize the dataset's likely trend, whereas trend analysis determines pattern and data consistency. Visualizing time series data patterns helps anticipate precipitation. Time series forecasting can predict future events if a pattern is present. Predicting seasonal behavior helps understand changing patterns and make forecasts. Visualizing time series data patterns has helped anticipate precipitation. Time series forecasting can predict future events if a pattern is present. Predicting seasonal behavior helps understand changing patterns and make forecasts (Chatfield, 2004).

Time series analysis was employed to analyze non-stationary data characterized by variables that exhibit temporal changes or are influenced by the passage of time. Seasonal pattern analysis was employed to comprehend the fluctuations in the MAM season pattern during a span of forty years. This particular sort of time series is highly suitable for analyzing the frequency of events that occur in sequence during the MAM (March, April, May) season. Time series analysis is a valuable tool for predicting weather patterns, aiding meteorologists in forecasting both short-term weather conditions and long-term climatic trends. Descriptive time series analysis can be employed to identify seasonal fluctuations.

### 3.2.1.4 Coefficient of variation of MAM seasonal rainfall

The Coefficient of Variation (CV) is a statistical measure that assesses the extent of dispersion or variability in relation to the mean. The percentage representation refers to the ratio of the standard deviation to the mean. A higher coefficient of variation signifies a larger deviation from the mean, while a lower coefficient of variation indicates a lesser deviation from the mean. Equation 3 is the mathematical expression used to compute the coefficient of variation (Hayes *et al.*, 2023.).

$$CV = \frac{\sigma}{\mu} * 100\% \dots \dots \dots (3)$$

In the Equation 3, The coefficient of variation (CV) represents the ratio of the standard deviation ( $\sigma$ ) to the mean ( $\mu$ ).

The CV was utilized in this work to examine the temporal fluctuations in MAM rainfall over the study region.

### 3.2.1.5 Mann-Kendall Trend test for significant test

The Mann-Kendall test was used to evaluate existence of statistically significant patterns in the time series of MAM (March-April-May) rainfall in the homogeneous zones of Kenya. Climate datasets can provide indications of long-term climatic changes through the use of non-parametric techniques to identify trends (Aditya *et al.*, 2021).

The Mann-Kendall (MK) test is used in this study to analyse variations in the lengthy rain seasons of Kenya's homogeneous zones and tropical cyclone data, as described in Equations 4 and 5. The MK test is used to evaluate whether the null hypothesis (Ho) should be accepted or rejected, and whether the alternative hypothesis (Ha) should be accepted, when there is a noticeable trend in a given dataset.

The null hypothesis states that there is no discernible pattern in the seasonal rainfall,

$$H_0: X_j = X_i, X_j - X_i = 0 \quad \text{No trend for null hypothesis}$$

And alternative hypothesis, there is a trend

$$H_a: X_j \neq X_i, X_j - X_i \neq 0 \quad \text{There is a trend for alternate hypothesis}$$

The Mann-Kendall test begins by assuming the null hypothesis (Ho) is true when there is no discernible trend in the data. Nevertheless, this hypothesis is refuted upon the identification of a pattern, resulting in the endorsement of the alternative hypothesis (Ha).

$$S = \sum_{i=1}^{n-1} \sum_{j=i+1}^n \text{sgn}(X_j - X_i) \dots \dots \dots (4)$$

Equation 4,  $\text{sgn}(X_j - X_i)$  is an indicator that takes the values 1, 0, or -1 as given by the sign of  $X_j - X_i$  that is:

$$\text{sgn}(X_j - X_i) = 1, \text{ if } X_j - X_i > 0$$

$$\text{sgn}(X_j - X_i) = 0, \text{ if } X_j - X_i = 0$$

$$\text{sgn}(X_j - X_i) = -1, \text{ if } X_j - X_i < 0$$



Equation 4, n is the number of years of the datasets and  $X_j$  are the sequential values.

The Mann-Kendall (MK) test method uses the following statistics:

$$Z = \begin{cases} 1 & \text{if } S > 0 \\ 0 & \text{if } S = 0 \\ -1 & \text{if } S < 0 \end{cases} \dots\dots\dots (5)$$

When S has a positive value, it can be deduced that the latest observation in the time series is generally larger than the previous data points. However, if S is a negative value, it can be noted that the subsequent time data series has a smaller magnitude than the preceding time data series. The Mann-Kendall (MK) test was used to evaluate statistical significance of the observed fluctuations in the seasonal rainfall patterns of the Monsoon Asia Monsoon (MAM) region. The analysis employed a significance threshold of 0.05 (P=0.05). The regions with p-values below 0.05 were found to have a statistically significant trend (Gitau *et al.*, 2013; Mueni, 2016).

**3.2.2 Determining Intra-Seasonal Variability and Trends in the Frequency of Tropical Cyclones North of 20°S and West of 60°E in the SWIO Region**

This study's goal was to examine the trends and variability in the occurrence of tropical cyclones in the southwest Indian Ocean region, with a particular emphasis on the region west of 60°E and north of 20°S. The accomplishment was attained through the execution of trend analysis on data pertaining to tropical cyclones. The analysis focused on both yearly and seasonal fluctuations within tropical cyclone datasets, with particular attention given to the graphical portrayal of these variations. This included an examination of the annual patterns observed in tropical cyclone activity. This procedure was conducted in order to ascertain the patterns and potential cyclic fluctuations observed throughout the years. The dataset was analyzed to determine the presence of seasonal fluctuation, which was subsequently linked to the long rain season in Kenya.

**3.2.3 Examination of the Potential Linkage of Frequency occurrence of Tropical Cyclones over SWIO region and MAM Seasonal Rainfall Kenya**

A Taylor diagram was employed to assess the correlation between Tropical cyclones and MAM rainfall in the uniform regions for this particular purpose. Four statistical measures were employed: Correlation analysis, Standard Deviation, Root Mean Square Error (RMSE), and model Bias. The MAM rainfall totals for the years 2006 and 2019 were assessed and contrasted with the average

rainfall for the same season over the study area from 1980 to 2019. The MAM season of 2006 and 2019 was chosen from the last twenty years of study period as they also experience positive IOD. Spatial and temporal analysis was used to show the distribution and patterns of change in these seasons. A brief description of these methods is described below.

#### **3.2.3.1 Tropical cyclone occurrence variability over the southwestern of the Indian Ocean**

Time series analysis is a technique for analyzing data points collected over a specific time period. It shows data points at regular intervals over a set time period (Pandian, 2021). An assessment was conducted to evaluate the link and performance of rainfall and tropical cyclones throughout the period of 1979 to 2019, using normalised values. The normalised values successfully exposed the years characterized by extreme values, as well as the patterns and cycles present over the whole time. Make a forecast or prediction of the target variable using the time variable as a point of reference. A time series is a chronological arrangement of orders organized by time, including years, months, weeks, days, hours, minutes, and seconds. This is a study of a series of discrete time intervals that occur one after the other (Pandian, 2021).

#### **3.2.3.2 Statistical evaluation of relation of tropical cyclone with March to May rainy season**

The Taylor diagram seen in Figure 3-2 offers a graphical depiction of the correlation between two variables or fields. The given visual depiction demonstrates the convergence of the correlation coefficient, Root Mean Square Error (RMSE), and standard deviation into a single data point. These statistics provide a concise overview of the connections between variables. This enables the assessment of the model's suitability in real-world systems for the aim of making predictions (Taylor, 2001).

The Taylor diagram was used to examine twelve homogeneous regions in Kenya to determine the correlation, standard deviation, and root mean square error of the occurrence of tropical cyclones over the Southwest Indian Ocean during the March-April-May seasonal rainfall period. A Taylor diagram, which effectively illustrates the degree of correlation and proximity between the rainfall values and the tropical cyclone data, can provide a more accurate depiction of the statistical data. The spatial arrangement of each data point indicates the degree of correlation between rainfall patterns and the presence of tropical cyclones. Proximity to the reference point signifies a stronger correlation between these variables. The aforementioned methodology has been employed to

ascertain the seasonal correlation between rainfall patterns and the incidence of tropical storms, thereby identifying the climatological region that experiences the most impact from these cyclonic disturbances. Equation 8 depicts the mathematical representation of the relationship illustrated in the Taylor diagram.

$$E^2 = \sigma_x^2 + \sigma_y^2 - 2\sigma_x\sigma_y r_{xy} \dots \dots \dots (6)$$

Equation 6, E is mean square error,  $\sigma_x$  is the standard deviation of MAM seasonal,  $\sigma_y$  the Standard deviation of frequency seasonal occurrence of tropical cyclones. Pearson correlation coefficient between the frequency of tropical cyclones occurrence and rainfall. The Pearson correlation is used as a measure the relatedness between the variables as the standard deviation and root mean square error are ratios.

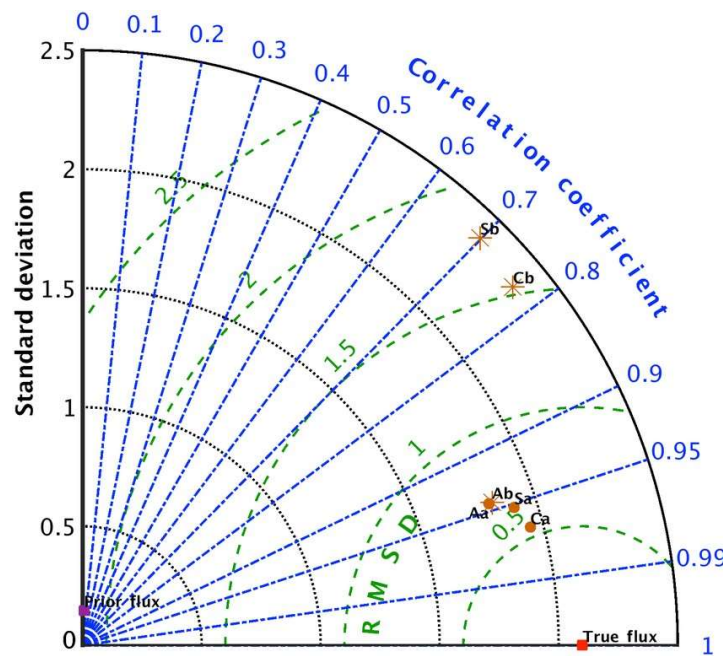


Figure 3-2: The Taylor diagram is depicted schematically for estimating standard deviation, root mean square error and Pearson correlation.

(Source: Taylor, 2001)

The correlation was instantaneous between season and season, lagging will mean going one year back which may not be significant as their other seasons in between.

### 3.2.3.3 Student test for significance of correlation between the variables

Student's t test, analysis of variance (ANOVA), and analysis of covariance (ANCOVA) are statistical techniques employed in hypothesis testing to compare the means of different groups. The Student's t test is employed for comparing means between two groups, whereas ANOVA is employed for comparing means among three or more groups. The P value is initially computed as a significant P value resulting from the ANOVA test, which shows that there is at least one pair for which the difference in means is statistically significant. The t-test is a parametric test used to determine differences between groups. It has the same assumptions about the data as other parametric tests. The t-test implies that your data is independent and follows a normal distribution, with approximately equal variance among each group being compared (Bevans, 2020).

The hypothesis interpretation:

The null hypothesis, no difference between the means of the two variables

Ho:  $\bar{x}_1 - \bar{x}_2 = 0$  , the difference between the means is equal to 0.

While the alternative hypothesis gives difference between the two variable is more than zero

Ha:  $\bar{x}_1 \neq \bar{x}_2$  ,  $\bar{x}_1 - \bar{x}_2 \neq 0$  , the difference between the means is more than zero

If the p-value is greater than the significance level of 0.05, then null hypothesis is accepted but if it is less than 0.05 significance level then alternate hypothesis is accepted.

Student test formula;

$$t = \frac{\bar{x}_1 - \bar{x}_2}{\sqrt{\left(\frac{s_1^2}{n} + \frac{s_2^2}{n}\right)}} \text{-----7}$$

In Equation 7, the variable t represents the student test, s1 and s2 represent the standard deviations, and n represents the number of degrees.

### 3.2.3.4 Comparison of Long Term Mean MAM Seasonal Rainfall to MAM Season of 2006 and 2019

Equation 7 is a simple question to calculate if there was deviation between the MAM seasonal rains of 2006 and 2019 from the Long-Term mean of MAM rainfall. MAM seasonal rains for 2019 were chosen due to notable cyclones (Idai and Kenneth) reported in mid-March and an increase in the cyclone of occurrences during that season of 2018/2019. These years were picked because they had one thing in common, they both experience positive Indian Ocean Dipole but different in terms of tropical cyclone occurrence.

$$D_{LTMSi} = \frac{(M_s - M_{LTM})}{M_{LTM}} * 100 \% \dots\dots\dots (8)$$

In Equation 7, the variable t represents the student test, s1 and s2 represent the standard deviations, and n represents the number of degrees

## CHAPTER FOUR

### 4.0 RESULTS AND DISCUSSION

#### 4.1 Results from Data Quality

Evaluating the quality of the observed records is crucial in any investigation. The homogeneity test was utilised to ascertain the consistency of data at each location. This study investigates the seasonal precipitation patterns and tropical cyclone data. The investigation of data consistency was performed using the single mass curve method. The graphs displayed demonstrate a significant level of coherence and uninterrupted flow in the data employed for the inquiry. This is seen by the almost straight paths shown. Upon examining the graphs presented in Figure 4-1, it becomes apparent that the data exhibits a high level of consistency. This is evident from the nearly linear nature of the graphs, which represent six stations located inside homogeneous zones 2,6 and 10. The single mass curve for homogenous Zones 5, 8 and 12, as depicted in Figure 4-2, has almost linear graphical representations. The datasets exhibited a consistent trend across all zones, suggesting a high level of quality and warranting their utilisation for subsequent study.

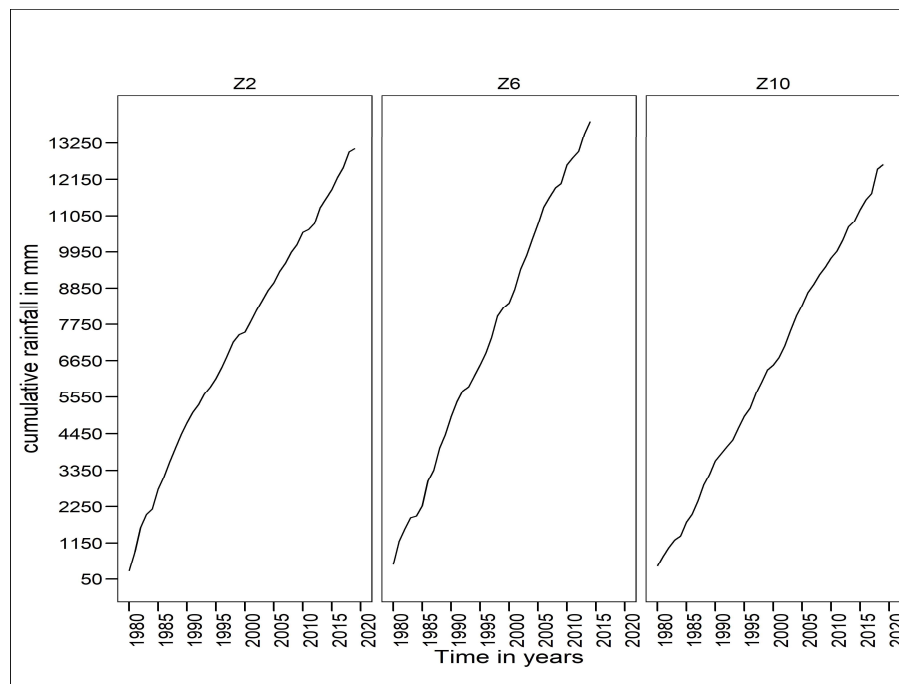


Figure 4-1: Single mass curves of cumulative MAM rainfall for homogeneous rainfall zones 2,6 and 10 of Kenya

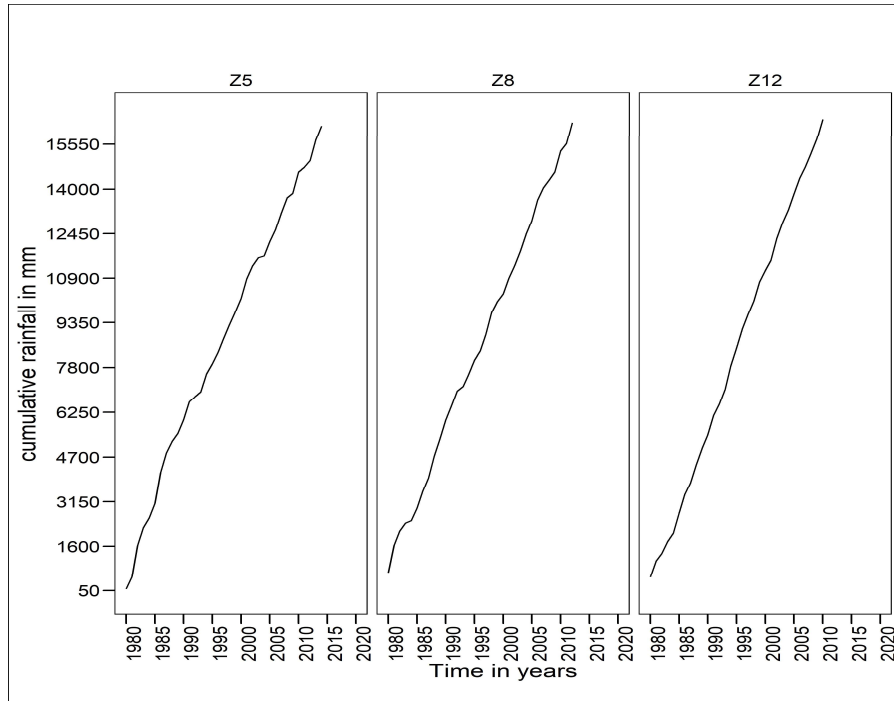


Figure 4-2: Single mass curves of cumulative MAM rainfall for homogeneous rainfall zones 5,8 and 12 of Kenya

## 4.2 Determination of Spatial and Temporal Distribution in MAM Seasonal Rains of Homogeneous Zones in Kenya

Various complex meteorological phenomena, operating at different scales from local to synoptic, display temporal and spatial dependence. These processes are essential in establishing the spatial and temporal distribution of MAM (March, April, May) rainfall within uniform regions in Kenya. The primary goal of this research was to investigate the spatial-temporal distribution of the MAM season in Kenya. The section that follows provides a summary of the findings from the analysis of rainfall patterns in the specified research region, including both space and time.

### 4.2.1 Spatial Distribution of MAM Seasonal Rains of the Homogeneous Zones in Kenya

The diagram in Figure 4-3 illustrates the geographical spread of rainfall in Kenya during the March-April-May (MAM) season. The Western region, Coastal zones (zones 5 and 6), and Dagoretti Corner station experience annual precipitation levels that surpass 406 mm (zone 8). The isohyet line illustrated in Figure 4-3 illustrates the presence of restricted rainfall in the ASAL region, particularly in Zone 1, Zone 2, Zone 3 (situated in the northwestern and northeastern areas of Kenya), and Zone 7 (including Voi and its surrounding areas). These locations see seasonal

precipitation ranging from 95 mm to 250 mm. The eastern areas of Kenya, specifically Zones 2 and 10, as well as the South Rift Valley region in Zone 10, had rainfall ranging from 302 mm to 406 mm during the season. The March-April-May seasonal rainfall is particularly concentrated in Zones 5, 6, 8, and 12, when the precipitation exceeds 400 mm. Conversely, other regions with uniform characteristics encounter diminished precipitation, which falls below the 400 mm benchmark. The arid and semi-arid zones, particularly Zone 1, 3, and 4, get the lowest precipitation levels throughout the MAM season, with an estimated 100 mm.

The spatial distribution analysis shows that the ASAL regions have uniform areas with a precipitation level of less than 300 mm every season. This limited amount of rainfall may prove insufficient for the cultivation of extended duration crops. This is appropriate for crops that have a short period to reach maturity and for pastoral practices. During the Monsoon Africa Model (MAM) season, precipitation above 300 millimeters is observed in the Western area, the south and central Rift Valley, and the coastal zone. These regions exhibit favorable conditions for rain-fed agricultural production.

According to the data presented in Figure 4-3, it was observed that almost two-thirds of the country experiences precipitation levels below 300mm, while only one-third of the homogenous zone receives rainfall beyond 300mm. Ayugi *et al.* (2016) conducted comparable investigations and observed variations in the MAM rainfall season across different regions in Kenya.



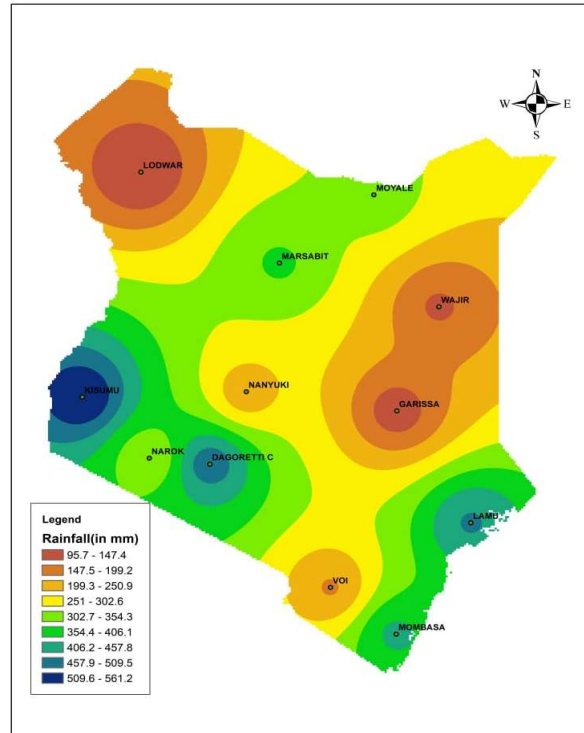


Figure 4-3: The spatial distribution of precipitation (measured in millimeters) in Kenya during the March-April season from 1980 to 2020 is depicted. The deep blue color represents areas with the most rainfall, while brown represents areas with the least.

#### 4.2.2 Temporal distribution of MAM seasonal rainfall data for homogeneous zones in Kenya

Time-series analysis was performed on data from March-April-May (Long rain season) seasonal rain anomalies in Kenya to assess patterns of trends and cycles in the data for the period 1980–2019. Figure 4-4 presents the time series data depicting the MAM seasonal rainfall patterns in the homogenous zones of Northern Kenya, specifically Lodwar, Moyale, and Wajir. These zones exhibit rainfall anomalies within the range of negative one standard deviation to positive one standard deviation (-1 to +1) during the majority of the analyzed period. This gives Upper Limit Standard deviation (ULT) and Lower Limit Standard deviation (LLT). The ASAL region experienced MAM seasonal rainfall below minus one standard deviation only in the years 2000 and 2010, resulting in the formation of homogenous zones. In both 2013 and 2018, all homogenous zones within the ASAL region had above-average over the upper standard deviation. Nevertheless, there was considerable variability in rainfall during the years, characterized by both above-average and below-average average MAM values for the duration of the study. From 1980 to 2020, the

region of Lodwar had six instances of above one positive standard deviation in rainfall, as well as three instances of below one negative standard deviation in seasonal rainfall. Moyale has five cases where the reported values were more than one standard deviation above and less than one standard deviation below the mean. Wajir saw six episodes of above-average positive one standard deviation seasonal rainfall in the MAM, as well as three episodes of rainfall below the lower standard deviation of -1. The MAM seasons in the ASAL regions were characterized by significant deviations from the average rainfall, with values either exceeding upper standard deviation limit of the mean or falling below the lower standard deviation limit. A quarter of the time, there are instances of high rainfall events that result in heightened precipitation exceeding one standard deviation, or there are periods of reduced seasonal rainfall leading to unsuccessful seasons.

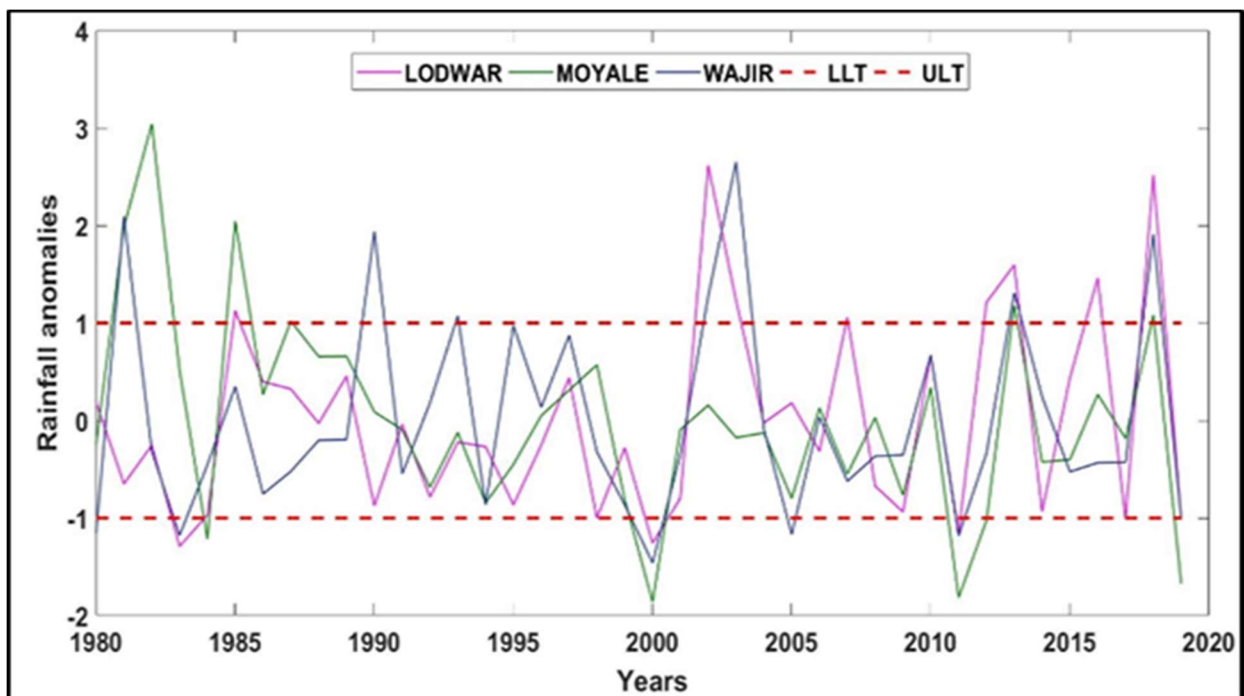


Figure 4-4: Rainfall anomalies during the March-April-May season were examined for three Kenyan stations: Lodwar, Moyale, and Wajir, from 1980 to 2019. Zone 1, Zone 2, and Zone 3 are represented by these stations.

The rainfall anomalies for the eastern and coastal regions, specifically the Garissa, Lamu, and Mombasa stations, are depicted in Figure 4-5. The Garissa station had a greater number of years falling within the standard deviation range, with the exception of 2018, during which it experienced exceptionally high levels of rainfall in comparison to other homogenous zones around

the country. The precipitation levels seen in the years 1993, 2005, and 2012 were found to be lower than the average range typically experienced during the corresponding seasons. The Mombasa station experienced above-average rainfall in the years 1982, 1986, 1998, 2001, 2014, 2016, and 2017. On the other hand, the years 1985, 1993, 2000, 2009, 2011, and 2012 exhibited a notable decrease in precipitation levels, falling below the average for the MAM seasons. In contrast, it was observed that Lamu and Mombasa stations experienced increased seasonal rainfall during the March-April-May period in 1983 and 1987, whereas a decrease in rainfall was observed during the same period in 2004.

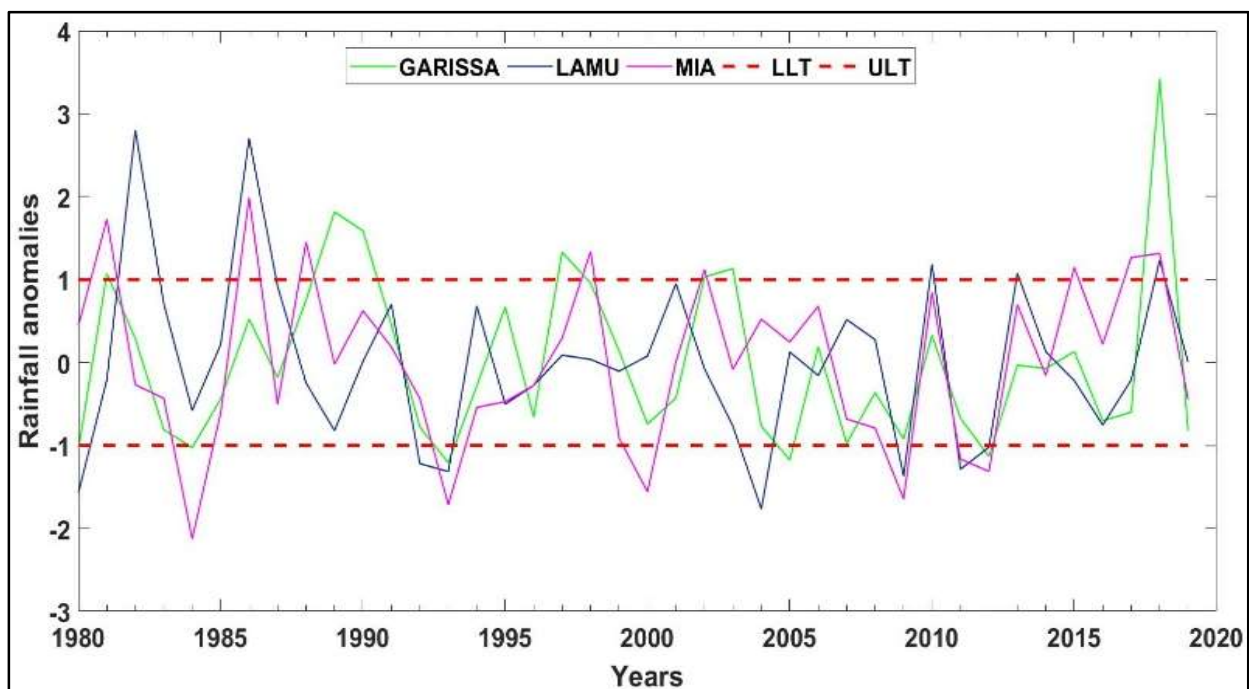


Figure 4-5: Rainfall anomalies for the March-April-May season between 1980 to 2019 for Garissa, Lamu and Moi international airport station representing zone4, zone 5 and zone 6 in Kenya

Figure 4-6 shows that MAM rainfall at all sites was within the normal range for most years. It rained a lot at Voi station in 1990, 1991, and 2010, which was above the normal amount for that time of year. Between 1980 and 2019, below-normal rainfall was recorded at the Dagoretti Corner weather station in zone 8. The wettest years for seasonal rainfall were 1984 and 1993. In 1981 and 2018, however, all sites had more rain than usual. In 1984 and 2000, it rained less than usual in Dagoretti Corner and Laikipia, which happened to be years when there was a drought.

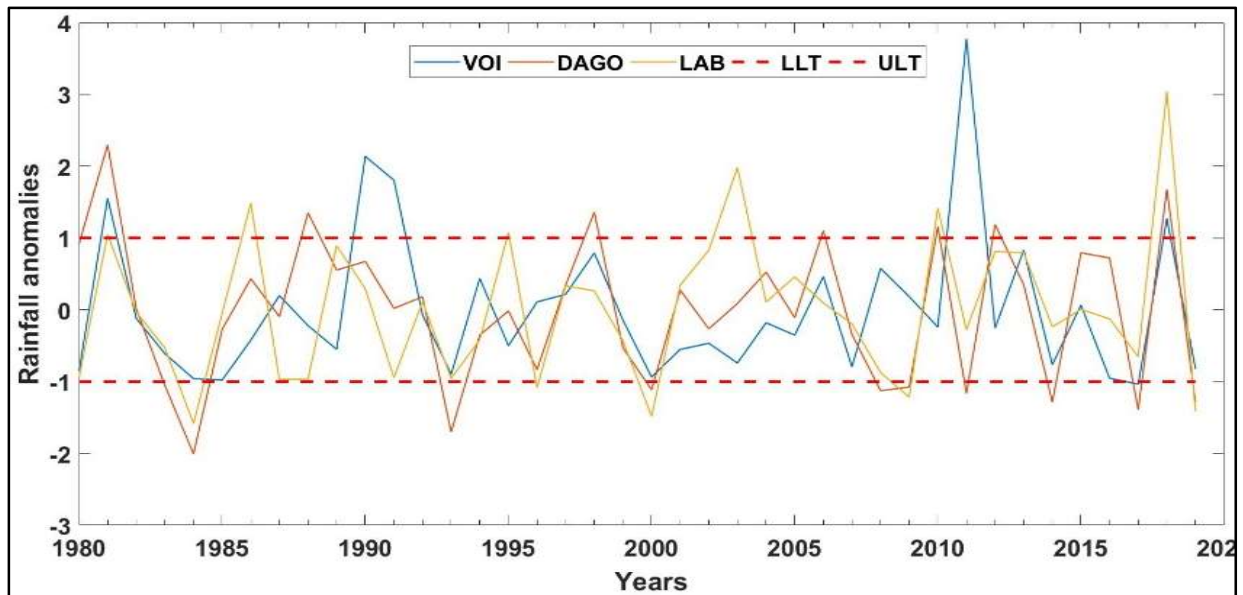


Figure 4-6: The rainfall anomalies during the March-April-May season from 1980 to 2019 were analyzed for three stations in Kenya, namely Voi, Dagoretti corner, and Nanyuki. These stations represent Zone 7, Zone 8, and Zone 9, respectively.

According to Figure 4-7, the year 2014 experienced the highest amount of precipitation in Kisumu station, while the next years exhibited average levels of rainfall. This particular station had significantly greater levels of precipitation in comparison to other stations located within the same geographical region throughout the period spanning from 1980 to 2019.

Hence, the results indicate that there is significant variability in rainfall patterns throughout the majority of homogenous zones. Notably, drought conditions were observed in almost all zones during the years 1984, 2000, and 2009, whereas increased rainfall was recorded in 1982, 1986/87, 1990, 2010, and 2018. The frequency of repeating enhanced events was seen to be higher than that of depressed rainfall events.

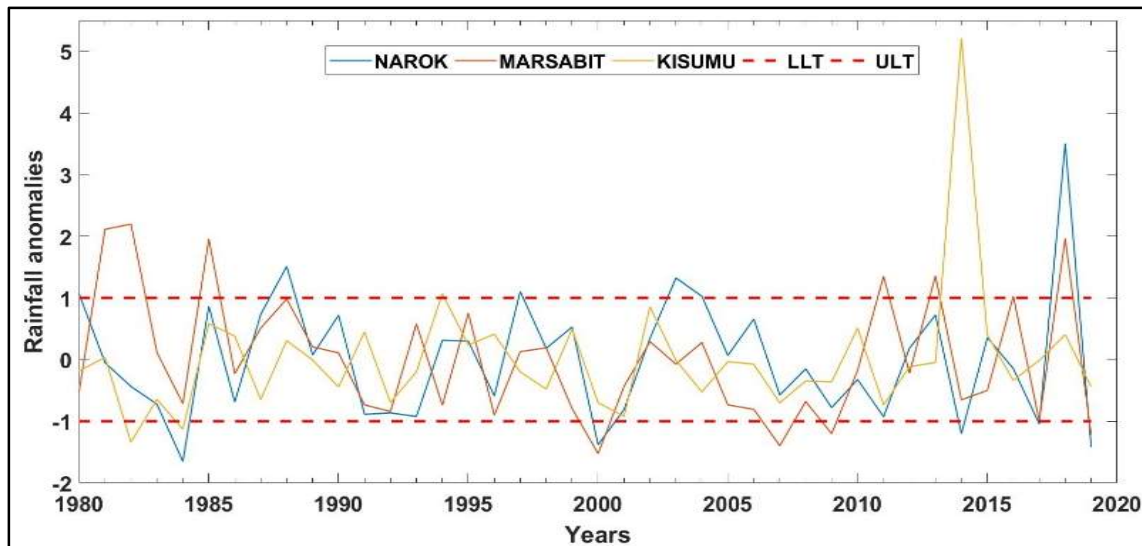


Figure 4-7: Rainfall anomalies for the March-April-May season between 1980 to 2019 for stations representing the homogeneous rainfall zones in Kenya

### 4.3 Determining the Intra-Seasonal Variability and Tendencies in the Frequency occurrence of Tropical Cyclones North of 20°S and West of 60°E in the SWIO Region

This section investigates the relationship between tropical cyclones in the Southwest Indian Ocean region and seasonal precipitation in Kenya during the months of March, April, and May. Time series analysis and spatial pattern evaluation were also used to assess the relationship between the occurrence of tropical cyclones and the long of the rainy season. Seasonal tropical cyclone data was analyzed to determine changes and patterns.

#### 4.3.1 Determining the Trends and the Intra-Seasonal Variability of Tropical Cyclones

Table 4-1 provides detailed monthly statistics on Tropical Cyclones that occurred between November 1979 and April 2019. These cyclones were observed within a geographical zone defined by the western limit of 60°E and the northern boundary of 20°S, which spans the Southwest Indian Ocean. Tropical cyclone activity is most common in the months of January, February, and March, and least common in November. According to Table 4-1, tropical cyclones in the Southwest Indian Ocean typically begin in November and end in April of the following year, with isolated occurrences documented during the other months. This data provides information on storm initiation and termination trends, allowing for a seasonal analysis of the region. According to the study's findings, tropical cyclones frequently form in the month of November, peak in strength in

the month of January, and then slowly decline until the month of April. The occurrence of cyclone activity in the Southern Hemisphere during a given period can be attributed to the sun's position, resulting in relatively high sea surface temperatures. This generates an ideal setting for cyclone development, resulting in cyclone activity maxima around this period. Water warms slowly once the Sun arrives at the Tropic of Capricorn in December due to its low conductivity. This phenomenon is visible since the cyclone's zenith occurs during the months of January and February.

Table 4-1: Tropical cyclone occurrence over the Southwestern of the Indian Ocean, 1979-2019

| <b>Months</b> | <b>Total tropical cyclone occurrence</b> |
|---------------|--|
| November      | 10                                       |
| December      | 37                                       |
| January       | 74                                       |
| February      | 66                                       |
| March         | 59                                       |
| April         | 27                                       |
| <b>TOTAL</b>  | <b>273</b>                               |

Figure 4-8 illustrates the temporal distribution of tropical cyclones in the Southwest Indian Ocean region, based on seasonal cyclone totals. Period of cyclone activity typically begins in November and ends in April, representing the approximate average annual occurrence of 7 (6.7) cyclones. This pattern is visually represented by a red horizontal line. The aforementioned time period aligns with the Sun's position in the Southern Hemisphere.

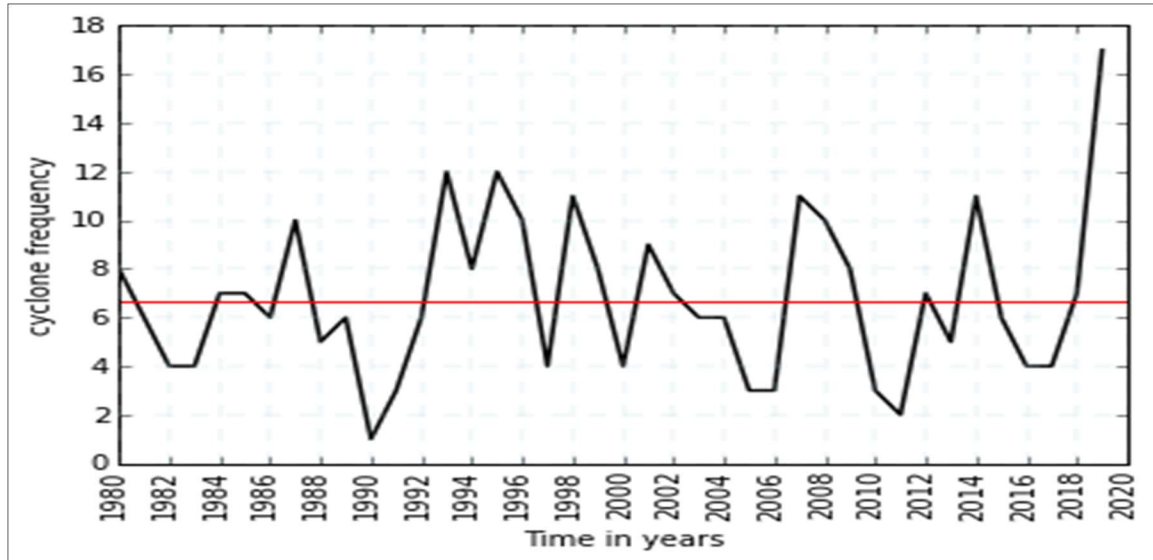


Figure 4-8: Cyclone frequency variation over the Southwestern of the Indian Ocean for the period 1980-2019

Figure 4-9 depicts the temporal distribution graph of tropical cyclones in the Southwest Indian Ocean region, using standard values. The dataset covers the time period from November 1979 to April 2019, clearly indicating a noticeable rising pattern. An investigation of seasons that deviate more than 1 standard deviation from the norm revealed the presence of intense cyclones. The frequency of intense storm episodes is rising, as seen by the significant increase in tropical cyclone events throughout the year 2018. From 1987 to 2011, inclusive, the number of recorded tropical cyclones was determined to be lower than the threshold of one standard deviation. The occurrence of tropical cyclones in the South-West Indian Ocean region showed a significant rise exceeding one standard deviation in the years 1988, 1994, 1996, 2007, and 2018. The frequency of tropical cyclone occurrences experienced a significant rise in the years 1994, 1996, and 2018 in comparison to the other years within the same time period. The increased frequency of tropical cyclones in the South-West Indian Ocean has had a negative impact on the amount of rainfall in the nearby region during the months of March, April, and May.



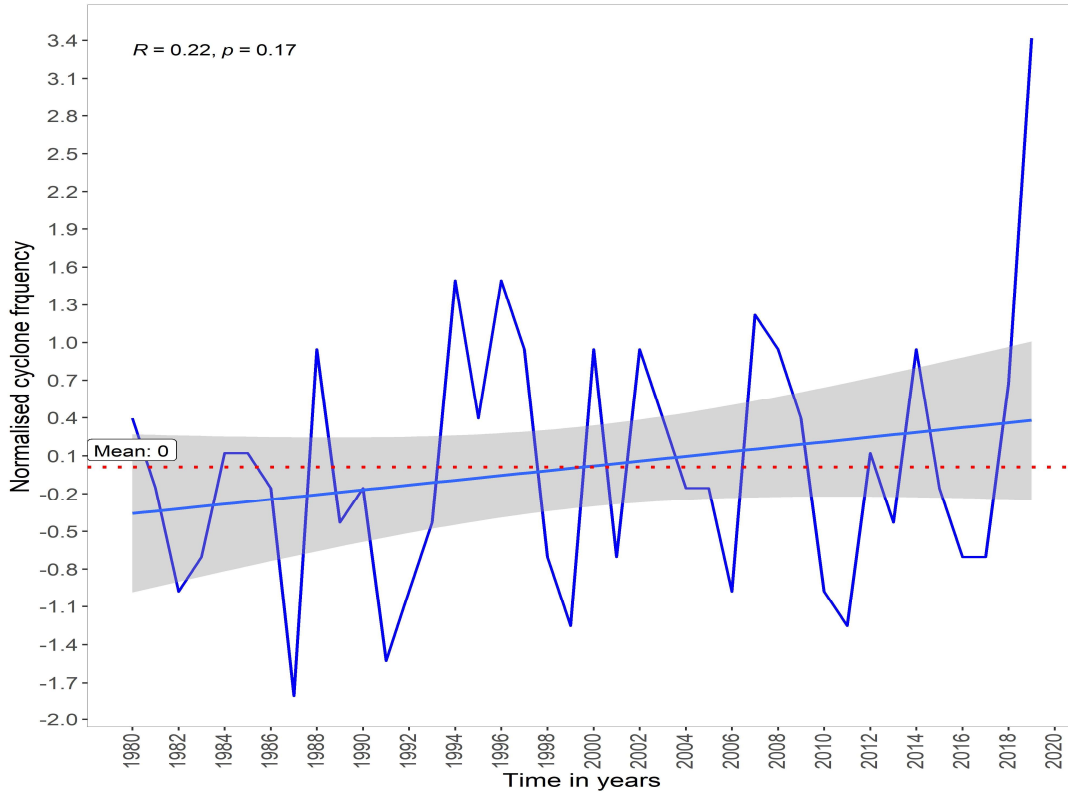


Figure 4-9: Cyclone frequency trend and inter-annual variation of tropical cyclones over SWIO from 1980 to 2019

#### 4.3.2 Temporal Variability and Trends in MAM Seasonal Precipitation

A Mann-Kendall test was conducted on the twelve homogeneous zones in Kenya to evaluate the temporal patterns and trends of MAM seasonal rainfall data. The data presented in Table 4-2 illustrates the results of the Mann-Kendall test conducted on rainfall stations situated within the study area, specifically focusing on the seasonal MAM rainfall.

The MK statistic quantifies the rate of change between two major points in a series as the line progresses in a left-to-right direction. The critical point at which the null hypothesis pertaining to a trend is either accepted or rejected. The determination of critical values is contingent upon the utilization of a test statistic that possesses a p-value below the threshold of 0.05. The Kendall correlation coefficient is a statistical metric that quantifies rate change of the slope. A positive one number indicates a perfect agreement in ranking, while a negative one value indicates a perfect disagreement with the rank. Kendall's Tau is a statistical metric which quantifies the degree of the



monotonic association between two variables, specifically in terms of their quantitative and ordinal correlation.

The observed changes for the majority of sites were found to be statistically insignificant throughout the March-April-May season. Nevertheless, it is worth noting that the Moyale station, located in zone 2, had a downward trend over the MAM season. This is evident from the Mann-Kendall statistic value of -2.0907, which is statistically significant with a Tau value below 0.05. The MAM seasonal precipitation shown a progressive decline throughout the period spanning from 1980 to 2019 in the regions of Wajir, Garissa, Lamu, Narok, and Marsabit, which correspond to Zones 3, 4, 5, 10, and 11. The Mann-Kendall statistical analysis yielded respective values of -0.035, -0.711, -0.152, -0.734, and -1.538 for these regions. At the 0.05 significant level, the Mann-Kendall statistic for Lodwar, Mombasa, Voi, Nanyuki, and Kisumu (Zones 1, 6, 7, 9, 12) were found to have small positive values of 0.501, 0.291, 0.082, 0.513, and 0.524, respectively.

Hence, the findings indicate that about ninety percent of the homogenous zones exhibit non-significant changing trends, except for Zone 2 (Moyale station), which has a significant trend with a Tau value of -2.097, falling below the threshold of 0.05. The gradual decrease in rainfall in Zone 2 is apparent.

Table 4-2: Tabulation of p-value and Kendall rank correlation (Tau) using seasonal rainfall for the 12 homogenous zones of Kenya

| <b>Mann-Kendall trend test</b> |             |                  |                |            |
|--------------------------------|-------------|------------------|----------------|------------|
|                                | <b>Zone</b> | <b>Mean (mm)</b> | <b>p-value</b> | <b>Tau</b> |
| <b>March-April-May (MAM)</b>   | Lodwar      | 95.6             | 0.308          | 0.501      |
|                                | Moyale      | 327.01           | <b>0.018</b>   | -2.097     |
|                                | Wajir       | 140.38           | 0.486          | -0.035     |
|                                | Garissa     | 119.46           | 0.239          | -0.711     |
|                                | Lamu        | 462.73           | 0.439          | -0.152     |
|                                | Mombasa     | 414.63           | 0.385          | 0.291      |
|                                | Voi         | 195.04           | 0.468          | 0.082      |
|                                | Dagoretti   | 491.3            | 0.284          | -0.571     |
|                                | Nanyuki     | 218.36           | 0.304          | 0.513      |
|                                | Narok       | 315.04           | 0.232          | -0.734     |
|                                | Marsabit    | 361.8            | 0.062          | -1.538     |
|                                | Kisumu      | 561.34           | 0.3            | 0.524      |

*\*Significant level=0.05*

### **4.3.3 The Coefficient of Variation in MAM seasonal Rainfall in Kenya**

Coefficient of variation is a statistical metric that measures the extent of variation in a dataset in relation to its mean within a sequence. The metric is derived by dividing the standard deviation by the mean and representing the outcome as a percentage. When data has larger coefficient of variation values, it shows a greater degree of dispersion from the mean. On the other hand, smaller CV values indicate a lesser or no dispersion from the mean.

Table 4-3 displays the documented variations in rainfall patterns across the geographic area of Kenya from 1980 to 2020. The regions of Lodwar, Wajir, Garissa, and Marsabit demonstrate high CV values, notably registering at 72%, 61%, 74%, and 74% respectively. The coefficient of variation for the ASAL is greater than 60%, which increases the likelihood of experiencing very variable seasonal precipitation. The ASAL zones are anticipated to have periods of heavy rainfall as a result of their substantial departure from the norm in terms of precipitation levels. The ASAL zones situated north of the equator mostly consist of Zones 1, 3, 4, and 11. The zones that displayed the greatest diversity in this investigation were zones 1, 3, 4, and 11. In contrast, zones 2, 5, 6, 7, 8, 9, and 12 exhibited a coefficient of variation of 53% or lower. Stations with high coefficient of variation are typically found in Arid and Semi-Arid Lands, which have dry and semi-arid conditions. These stations are naturally more prone to uncertainty throughout the March-April-May season.

Table 4-3: Mean, standard deviation, and coefficient of variation of rainfall over Kenya for the March-April-May season

|                              | <b>Variability of Rainfall (mm)</b> |             |                           |                                     |
|------------------------------|-------------------------------------|-------------|---------------------------|-------------------------------------|
|                              | <b>Zone</b>                         | <b>Mean</b> | <b>Standard Deviation</b> | <b>Coefficient of Variation (%)</b> |
| <b>March-April-May (MAM)</b> | Lodwar                              | 95.6        | 68.54                     | <b>72</b>                           |
|                              | Moyale                              | 327.01      | 132.93                    | 41                                  |
|                              | Wajir                               | 140.38      | 85.04                     | <b>61</b>                           |
|                              | Garissa                             | 119.46      | 88.56                     | <b>74</b>                           |
|                              | Lamu                                | 462.73      | 227.75                    | 49                                  |
|                              | Mombasa                             | 414.63      | 170.31                    | 41                                  |
|                              | Voi                                 | 195.04      | 102.97                    | 53                                  |
|                              | Dagoretti                           | 491.3       | 200.96                    | 41                                  |
|                              | Nanyuki                             | 218.36      | 100.97                    | 46                                  |
|                              | Narok                               | 315.04      | 119.13                    | 38                                  |
|                              | Marsabit                            | 361.8       | 228.78                    | <b>63</b>                           |
|                              | Kisumu                              | 561.34      | 228.95                    | 41                                  |

**Figure 4-10** illustrates the geographical arrangement of the coefficient of variation. The figure clearly shows that zones 1, 3, 4, and 11 have values exceeding 55%, showing a significant display of variation among the various zones. Furthermore, it highlights the significant departure from the norm. The cumulative value for the other zones, specifically Zones 2, 3, 4, 6, 7, 8, 9, 10, and 12, demonstrates a percentage that is less than 55%. This phenomenon can be observed in the geographical areas surrounding the town of Lodwar in the northwest, the upper eastern region around Marsabit, and the northeastern region encompassing Garissa. The high coefficient of variation observed in the Arid and Semi-Arid Lands region indicates that the occurrence of the MAM seasons in these locations is inconsistent, and there is a significant probability of failed seasons. The MAM season in the ASAL zones is marked by a significant degree of volatility. The Northwestern, Northeastern, Eastern, Upper Eastern, and Central regions of Kenya have substantial coefficients of variation, which together account for almost 58% of the overall seasonal rainfall.

Therefore, this study's results indicate that the zones in the Arid and Semi-Arid region have coefficient of variation values that are greater than 60%, whereas 40% of the homogeneous zones

show lesser variability. The Arid and Semi-Arid regions exhibit an uncertain MAM rainfall season, which distinguishes them from other homogeneous zones. This observation highlights the unreliability of seasonal precipitation in these regions, as evidenced by a significant deviation from the average seasonal rainfall.

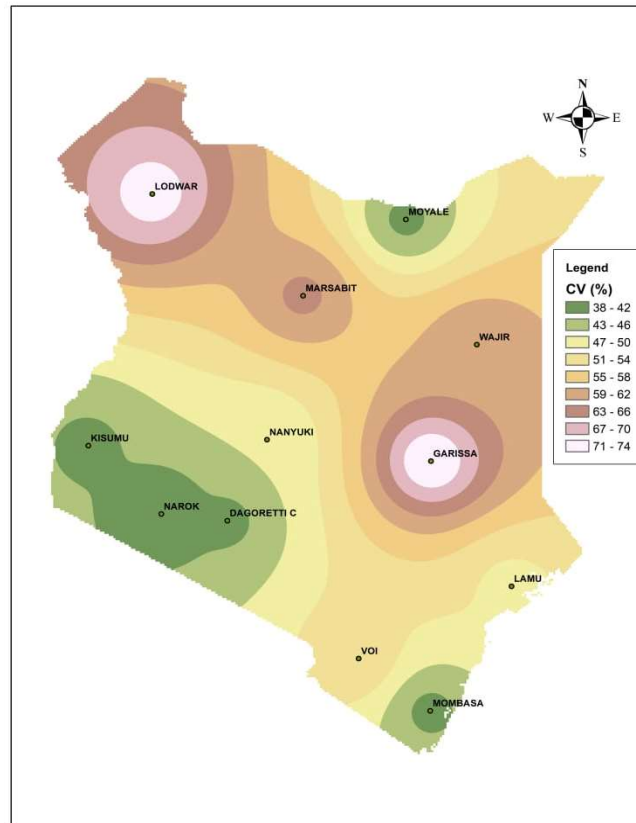


Figure 4-10: Spatial distribution of Coefficient of Variation in percentage (%) of the March-April-May rains over Kenya based on data, 1979-2019.

#### 4.4 Examination of the Potential Linkage of Frequency occurrence of Tropical Cyclones over SWIO region and MAM Seasonal Rainfall Kenya

This subsection will analyze the time series data about tropical cyclones and MAM (March-April-May) rainfall. The study aims to investigate the relationship between tropical cyclones over the Southwest Indian Ocean region with MAM seasonal rainfall. This will be done using the Taylor diagram. Moreover, it will examine the correlation between the frequency of the tropical cyclone occurrence with MAM seasonal precipitation in the season of 2005/2006 and 2018/2019. Conduct a comparison of the long-term MAM seasonal rainfall patterns and do an analysis of the MAM seasons between 2006 and 2019.

#### 4.4.1 Temporal Distribution of Tropical Cyclone and MAM Rainfall

Figure 4-11 presents a time trend illustrating the frequency of tropical cyclones in March, coupled with the MAM rainfall data for twelve uniform zones. The figures indicate that when the occurrence of tropical cyclones surpassed one positive standard deviation, indicating a high frequency of cyclones, there was a negative effect on the seasonal rainfall. Concretely, this pattern was noted in the years 1993, 2008, 2014, and 2019. During these time periods, most areas witnessed a decrease in seasonal precipitation, although a few areas were minimally impacted.

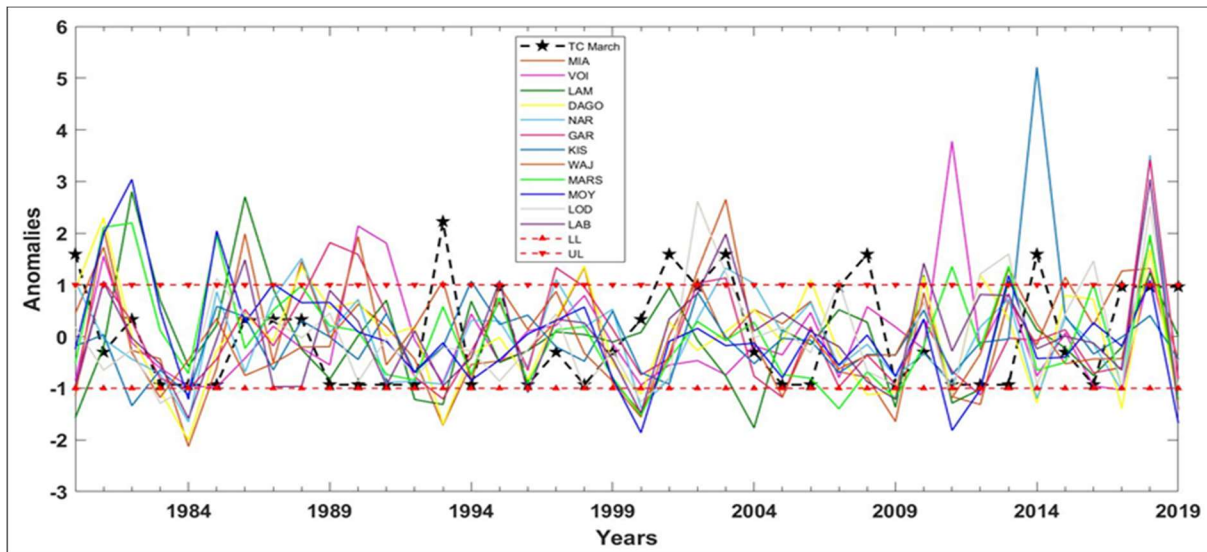


Figure 4-11: Time series graphs shows the tropical cyclone occurrence in March over the SWIO with the MAM seasonal rainfall for homogeneous Zones

Figure 4-12 presents a time series analysis of tropical cyclones in relation to the MAM seasonal rainfall pattern. The graph displays data on the frequency of tropical cyclones in the South-West Indian Ocean region, specifically in connection to the seasonal precipitation during the months of March, April, and May. The dataset comprises data collected from numerous representative stations situated within homogeneous zones. The findings suggest that the country witnessed heightened levels of seasonal precipitation during periods of low tropical storm occurrence, while encountering diminished amounts of seasonal rainfall during periods of frequent tropical cyclone activity. Figure 4-12 shows that precipitation was lower than the long-term average for the corresponding seasons in 1993, 1995, 1998, 2001, 2003, 2008, 2014, and 2019. The decrease in precipitation coincided with an increase in the occurrence of tropical cyclones. As a result, the

amount of seasonal precipitation decreased during years with a high occurrence of storms in the south-west Indian Ocean region. However, precipitation between 1984 and 2000 was significantly below average, falling below zero. It's worth noting that this decrease in rainfall was not caused by a tropical storm, as it stayed within the acceptable range of variation. The country experienced a period of intense drought lasting two years, which had a widespread impact. This indicates the presence of different atmospheric systems that regulate precipitation in Kenya.

In 1993, 1995, 2014, and 2019, there was a reported increase in the frequency of tropical cyclones, which was linked to decreased precipitation and a higher incidence of tropical cyclones in uniform areas. When compared to other zones that are similar, the effects of the Kisumu Meteorological Station, which is located in Zone 12 of the Western area, and the Lamu Meteorological Station, which is located in Zone 5 of the Northern coastal region, were relatively minor. 2019 saw an increase in the frequency of tropical cyclones, and all weather stations recorded below-average precipitation levels during that year. This happened in a season characterized by gloomy weather patterns. The seasons exhibiting the most substantial quantities of precipitation in the months of March, April, and May were recorded in the years 1982, 1986, 1990, 1998, 2006, 2010, 2013, 2016, and 2018. Significantly, these seasons aligned with periods when the average frequency of tropical cyclones occurred during the specified span.

According to a study conducted by Muthoni *et al.*, (2019), the occurrence of heightened cyclonic activity in the Indian Ocean had varying impacts on seasonal precipitation across different regions in Eastern and Southern Africa.

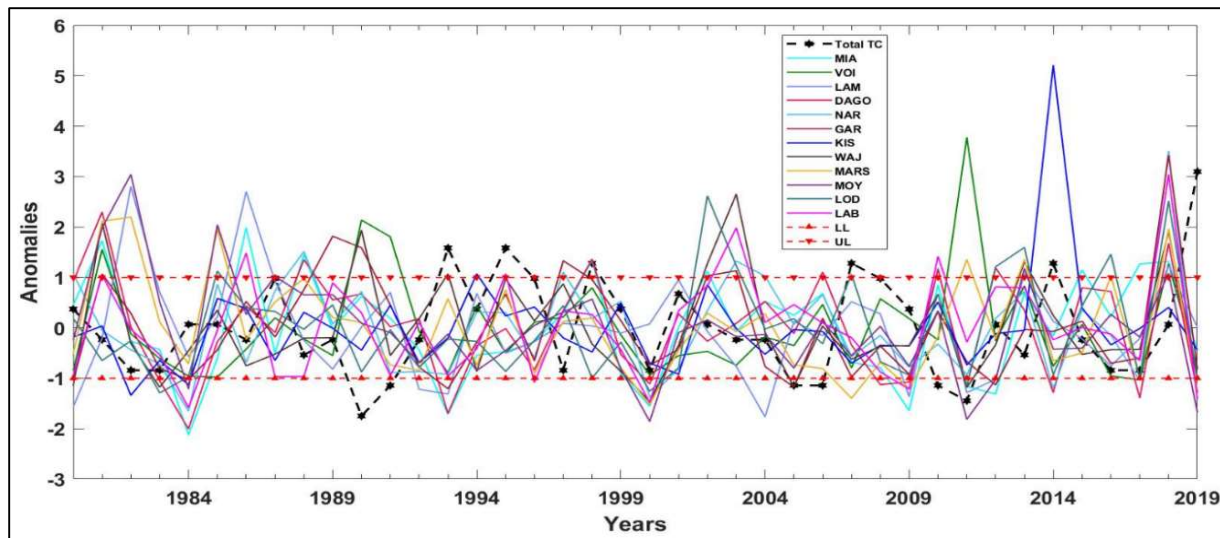


Figure 4-12: Time series graphs shows the Tropical Cyclone occurrence (TCs seasonal occurrence) over the SWIO against the MAM seasonal rainfall for homogeneous Zones.

Hence, these findings demonstrate a correlation between the frequency of cyclone occurrences and the overall precipitation levels during a given season. Specifically, a higher number of tropical cyclone occurrences have a detrimental impact on the amount of rainfall received, whereas fewer or no occurrences of tropical cyclones are conducive to an increased volume of rainfall throughout the season. There is a clear indication that the MAM season is likely to experience a decrease in precipitation levels.

#### 4.4.2 Examine link of Tropical Cyclone occurrence over the southwestern of the Indian Ocean region to March-April-May Seasonal Rainfall in Kenya

Time series analysis is a statistical technique employed to evaluate the fluctuations in tropical cyclones over a period of forty years. Taylor diagrams are used to investigate the possible relationship between seasonal rainfall and tropical cyclones in the southwestern part of the Indian Ocean. This is done by analyzing correlations, standard deviation, and root mean square error. The Taylor diagram displays the correlation, standard deviation, and root mean error values for tropical cyclones in the southwestern region of the Indian Ocean and the seasonal precipitation during March, April, and May. The Taylor diagram provides a graphical depiction of the correlation between tropical cyclones and the patterns of seasonal precipitation in Kenya. Furthermore, it

identified the homogeneous regions that experienced the greatest influence from these cyclonic occurrences.

According to the data presented in Figure 4-13, there is a negative correlation between tropical cyclone occurrence in the month of February and the March-April-May seasonal precipitation in ten out of the twelve homogenous zones. There was a little positive association seen between Zone 5 (Lamu station) and Zone 12 (Kisumu station). The range of the standard deviation was observed to be 0.74 to 1.1, while the root mean square error ranged from 1.2 to 1.6.

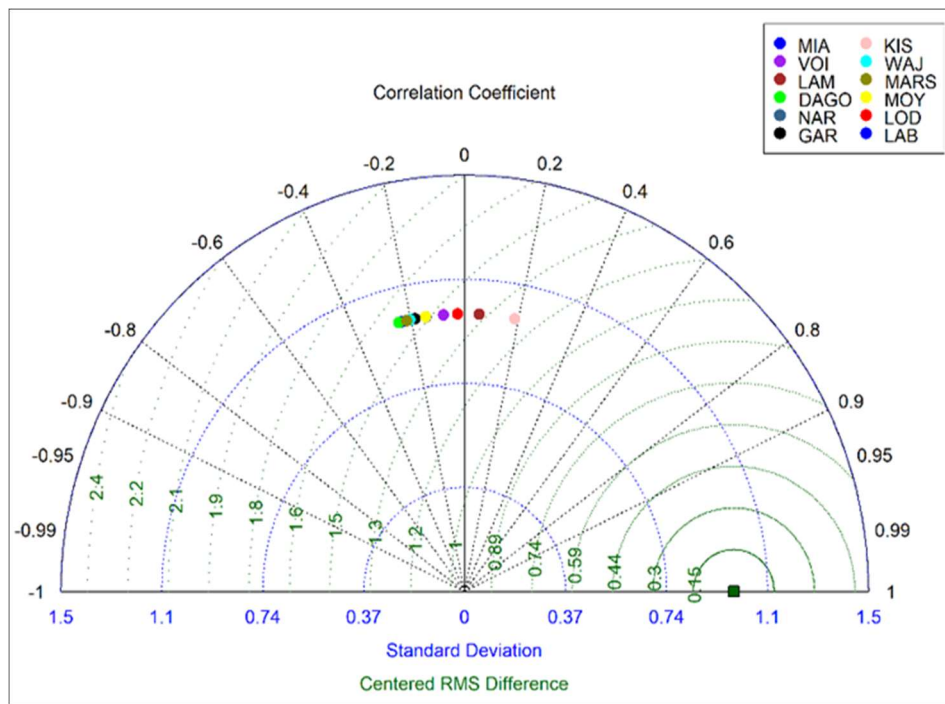


Figure 4-13: The Taylor diagram illustrates Pearson correlation, root mean square error, and standard deviation between the occurrence of tropical cyclones in February and the seasonal rainfall in Kenya during March, April, and May..

Figure 4-14 illustrates that the presence of tropical cyclones in March has a detrimental effect on the seasonal rainfall throughout the months of March, April, and May in almost 50% of the homogenous zones. There are six zones that exhibit a negative correlation ranging from zero to -0.4, while another six zones demonstrate a positive correlation ranging from zero to 0.2. The standard deviation of the zones varied from 0.74 to 1.1, while the root mean square error for the zones ranged from 1.2 to 1.6.



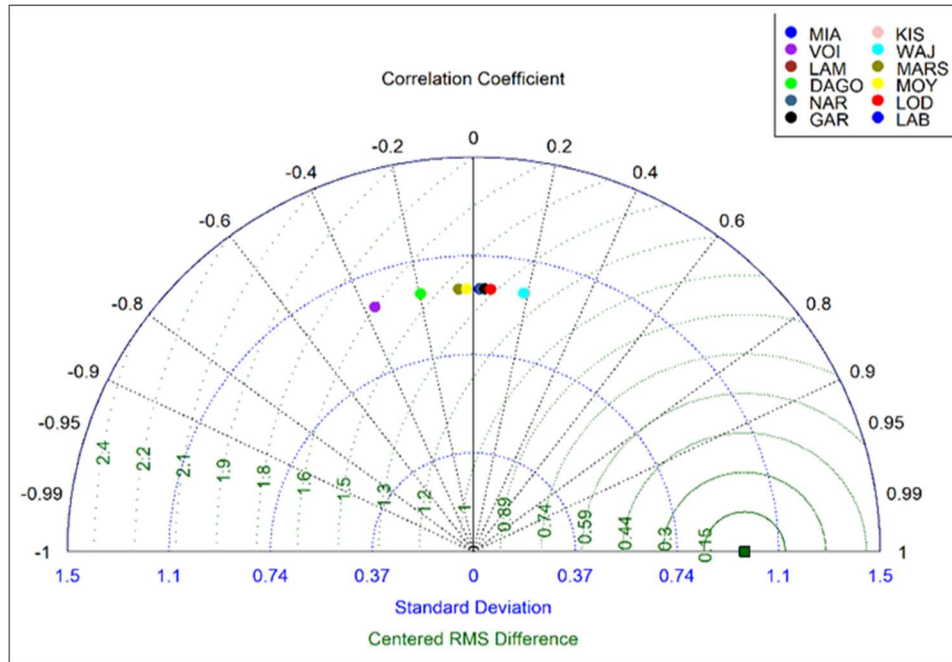


Figure 4-14: Taylor diagram displaying Pearson correlation, root mean square error, and standard deviation between March tropical cyclone with the March-April-May seasonal rainfall in Kenya.

The Taylor diagram methodology was used to illustrate the link between tropical cyclones and March-April-May seasonal precipitation in Kenya from 1980 to 2019. This is shown in Figure 4-15. The analysis indicates an inverse relationship between the seasonal rains occurring in March, April, and May and occurrence of tropical cyclones in eight of the twelve zones. The towns of Lodwar, Moyale, Wajir, Garissa, Voi, Dagoretti Corner, Nanyuki, and Marsabit, situated in Zones 1, 2, 3, 4, 7, 8, 9, and 11 respectively, demonstrate a negative correlation ranging from -0.05 to approximately -0.3 between their seasonal rainfall during March-April-May period and occurrence of tropical cyclones in the Southwest Indian Ocean region. The findings suggest that there is a negative relationship between tropical cyclones and rainfall during months of March, April, and May in the indicated regions. This statement emphasizes the importance of closely monitoring and efficiently mitigating the effects of tropical cyclones in these areas. The relationship between tropical cyclones and March-April-May rainfall is weak, as seen by the root mean square error, which ranges from 1.2 to 1.6. Kisumu station designates Zone 12, which includes the Lake Victoria region and its adjacent territories. The correlation coefficient in this zone is roughly +0.2, indicating a positive relationship. The observation root mean square error for tropical cyclones is 1.2, while the standard deviation is approximately 0.9. The stations situated in Zone 5, Zone 6, and

Zone 7 along the coastline region have a correlation coefficient close to zero (0), indicating a negligible connection with the increased frequency of tropical storms in the Southwestern Indian Ocean region. The root mean square error values show a significant increase, ranging from 1.3 to 1.6 units above the reference point, where the root mean square error value is zero. Nevertheless, these values exhibit a scattered distribution, deviating substantially from the central point.

The standard deviation of March-April-May precipitation from typical stations in zone 12 varies between 0.7 and 1.0. However, the standard deviation of tropical cyclone precipitation is roughly 1. The standard deviation of the zones varies between 0.75 and 1.1, much like Tropical Cyclones.

Therefore, the above-mentioned results indicate that the increased occurrence of tropical cyclones in the southwestern region of the Indian Ocean in the month before the season affects the total amount of rainfall during the season. Therefore, it is clear that a higher frequency of tropical cyclones during the season will impact the amount of rainfall experienced in the months of March-April-May.

Zhu and Quiring, (2022) conducted a study that examined the impact of heightened cyclone activity on precipitation patterns in the United States. Their findings indicated a notable increase in rainfall as a result of this phenomenon. Yoshida and Itoh (2012) conducted a study that demonstrated the capacity of cyclones, specifically typhoons, to elicit an indirect impact on the seasonal precipitation patterns within a certain geographical area.

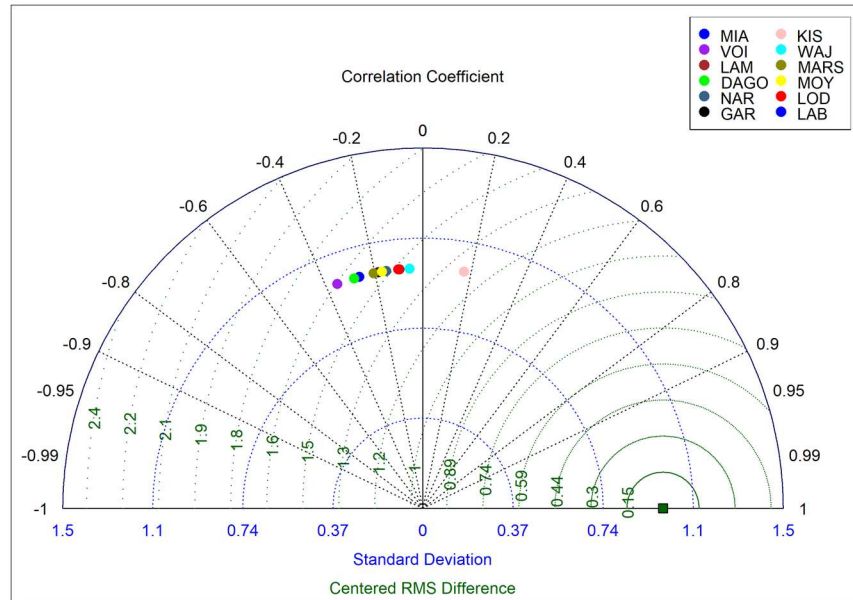


Figure 4-15: Taylor diagram displaying Pearson correlation, root mean square error, and standard deviation between Seasonal Tropical Cyclones with March-April-May seasonal rainfall in Kenya.

Consequently, the aforementioned findings suggest that the heightened occurrence of tropical cyclones during the month preceding a given season has an impact on the cumulative precipitation levels throughout that season. The negative impact of a high frequency of tropical storms occurring in close proximity to March-April-May season on rainfall patterns is evident.

#### 4.4.2.1 Significance test for correlation between Tropical cyclone occurrence with the MAM seasonal rainfall

Figure 4-4 shows the calculated values of correlation between tropical cyclones over southwestern of the Indian Ocean with March-April-May rainfall, the Student test results and the P-values for testing significance of the relation between tropical cyclones with March-April-May rainfall. All the homogeneous zones had t-test of less than significance level of 0.05 and seven out of twelve homogeneous zones showed significant relatedness of tropical cyclone occurrence and the performance of March-April-May seasonal rainfall as it had p-values less than significance level of 0.05. This was tested at confident interval at 95% showing the means of the tropical are not the same and the residual not follow normal distribution. The zones which have significantly affected with the occurrence of tropical cyclones over the SWIO are zone 1, zone 3, zone 4, zone 7, zone 10, zone 11 and zone 12 as indicated in the Table 4-4.



Table 4-4: the calculated correlation and Student tests result showing t test and p-values

|    | Station   | Pearson Correlation | p-value        | t test |
|----|-----------|---------------------|----------------|--------|
| 1  | Lodwar    | 0.05                | <b>0.00661</b> | 0.048  |
| 2  | Moyale    | -0.289              | 0.10440        | 0.048  |
| 3  | Wajir     | 0.041               | <b>0.00422</b> | 0.048  |
| 4  | Garissa   | -0.018              | <b>0.00213</b> | 0.048  |
| 5  | Lamu      | -0.081              | 0.05522        | 0.048  |
| 6  | MIA       | -0.084              | 0.87942        | 0.048  |
| 7  | Voi       | -0.275              | <b>0.00003</b> | 0.048  |
| 8  | Dagoretti | -0.205              | 0.84206        | 0.047  |
| 9  | LAB       | -0.13               | 0.15457        | 0.047  |
| 10 | Narok     | 0.01                | <b>0.02967</b> | 0.048  |
| 11 | Marsabit  | -0.268              | <b>0.01730</b> | 0.048  |
| 12 | Kisumu    | 0.227               | <b>0.00000</b> | 0.048  |

**95% confidence interval on the difference between the means**

#### **4.4.3 Link between extreme occurrence of Tropical Cyclones over southwestern of Indian Ocean and performance during the 2006 and 2019 March-April-May Seasons**

To assess the influence of the abnormally frequent tropical storms in the South-West Indian Ocean area during the cyclone seasons of 2005/2006 and 2018/2019 on the seasonal rainfall patterns in March, April, and May. The spatial distribution plots of the average March-April-May seasonal rainfall were compared to the March-April-May season of 2006, which had a low occurrence of tropical cyclones, and the March-April-May season of 2019, which had a high occurrence of tropical cyclones in the Southwest Indian Ocean region. The years 2006 and 2019 were selected for comparison because of the observed decrease in the latter half of the dataset over the past 20 years. They have up-to-date expertise, allowing them to offer a precise report on the current developments in Kenya.

Table 4-5 displays the mean rainfall for the months of March, April, and May, as well as the rainfall during the same period in the years 2006 and 2019. The table additionally displays the % departure of recorded rainfall from the average rainfall over a long period of time. In 2006, the occurrence of tropical cyclones in the southwest region of the Indian Ocean was infrequent, with a total of three recorded. Most areas with consistent rainfall patterns experienced positive percentage deviations, suggesting a rise in precipitation. Nevertheless, four clearly delineated homogeneous

zones (Zones 1, 8, 11, and 12) deviated from this pattern and had negative deviations, signifying a decrease in rainfall. Zone 11 had the most significant decrease with a negative percentage change of -51%, while Zones 1, 8, and 12 had negative percentage changes of -23%, -8%, and -3%, respectively. Conversely, most areas saw below-average MAM rainfall in 2019, which coincided with a significant number of tropical cyclones (17). Nevertheless, Lamu Station (Zone 5), Mombasa Station (Zone 6), and Kisumu Station (Zone 12) experienced a slight increase of approximately 18%. Significantly, this time period coincided with a substantial surge in the frequency of tropical cyclones in the southwestern region of the Indian Ocean. The MAM (March-April-May) season of 2006 had a higher amount of rainfall compared to the MAM season of 2019, which had a lower amount of rainfall than the average over a lengthy period of time. With the exception of Zone 5 (Lamu Station), the majority of zones had negative deviations from the average. Table 4-4 demonstrates that Zones 1, 11, and 12 consistently exhibited a negative deviation, regardless of the frequency of cyclone events in the southern Indian Ocean. This observation suggests that, apart from the influence of the frequent occurrence of tropical cyclones, there is another meteorological factor that contributes to the adverse deviation in the three zones. The impacted areas are precisely located to the north of the equator and to the west of the longitude 36° E. A discernible pattern is apparent. Forecasting relies on the understanding of shifting patterns throughout time, which is facilitated by predicting seasonal behavior. Utilizing visual representations to analyze patterns in time series data has demonstrated to be a valuable instrument in forecasting the occurrence of precipitation. Time series forecasting is a reliable approach for predicting future events when there is a noticeable trend. Forecasting relies on the understanding of shifting patterns throughout time, which is facilitated by predicting seasonal behavior.

Table 4-5:: Comparison between MAM long term mean (LTM) rainfall, MAM of 2006 and the MAM of 2019 season

| Station          | MAM LTM (mm) | MAM2006 (mm) | MAM2019 (mm) | % dev2006 | % dev2019 |
|------------------|--------------|--------------|--------------|-----------|-----------|
| Lodwar           | 95.7         | 74           | 25.9         | -23       | -73       |
| Moyale           | 327.0        | 344.1        | 104.5        | 5         | -68       |
| Wajir            | 140.4        | 143.3        | 54.5         | 2         | -61       |
| Garissa          | 119.5        | 136.1        | 46.7         | 14        | -61       |
| Lamu             | 462.73       | 427.3        | 464.0        | -8        | +0.3      |
| Mombasa          | 414.6        | 530.5        | 338.9        | 28        | -18       |
| Voi              | 195.0        | 242.7        | 110.3        | 24        | -43       |
| Dagoretti corner | 491.3        | 713.1        | 232.6        | 45        | -53       |
| Nanyuki          | 218.4        | 228.1        | 75.5         | 5         | -65       |
| Narok            | 315.0        | 393.3        | 145.6        | 25        | -54       |
| Marsabit         | 361.8        | 177.1        | 82.0         | -51       | -77       |
| Kisumu           | 561.3        | 544.1        | 460.5        | -3        | -18       |

Figure 4-16 depicts spatial coverage of MAM seasonal rainfall in percentage difference from long-term mean for the MAM season rainfall of 2006 and 2019.

According to **Figure 4-16 a**, there was an increase in seasonal rainfall in 2006 throughout the majority of homogenous zones that experienced low or no tropical cyclone activity. The majority of homogeneous zones exhibited a positive percentage departure in seasonal rainfall. However, three specific homogeneous zones (Zone 1, 5, and 11) demonstrated a deviation ranging from -8% to -55%.

**Figure 4-16 b** illustrates the Multi-Agency Malaria Model data for the year 2019, revealing a notable decrease in the rainfall during MAM season across the majority of zones. The data indicates that a majority of the geographical areas in the country saw below-average long-term precipitation, with the Arid and Semi-Arid Lands region exhibiting a negative deviation of 60% from the Mean Annual Maximum seasonal rainfall. In the context of the 2019 MAM season, the zones that experienced the greatest impact were identified as Zones 1 (Lodwar station), 2 (Moyale station), 3 (Wajir), 4 (Garissa station), 9 (Nanyuki station), and 11 (Marsabit station). The percentage deviation between the mean seasonal precipitation of 2019 and long-term mean MAM in Zones 7, 8, and 10 exhibited a negative deviation ranging from 40% to 59%. Conversely, in

Zones 5, 6, and 12, the negative deviation ranged from 0% to 19%, while the surrounding areas experienced a negative deviation ranging from 20% to 39%. During the 2019 MAM season, a significant majority of the country, specifically over 80%, had negative deviation. This negative deviation was particularly pronounced in 9 out of the 12 zones, where it exceeded 30%. In comparison, during 2006 MAM season, 9 out of the 12 zones exhibited deviation ranging from negative five to positive forty-five percent.

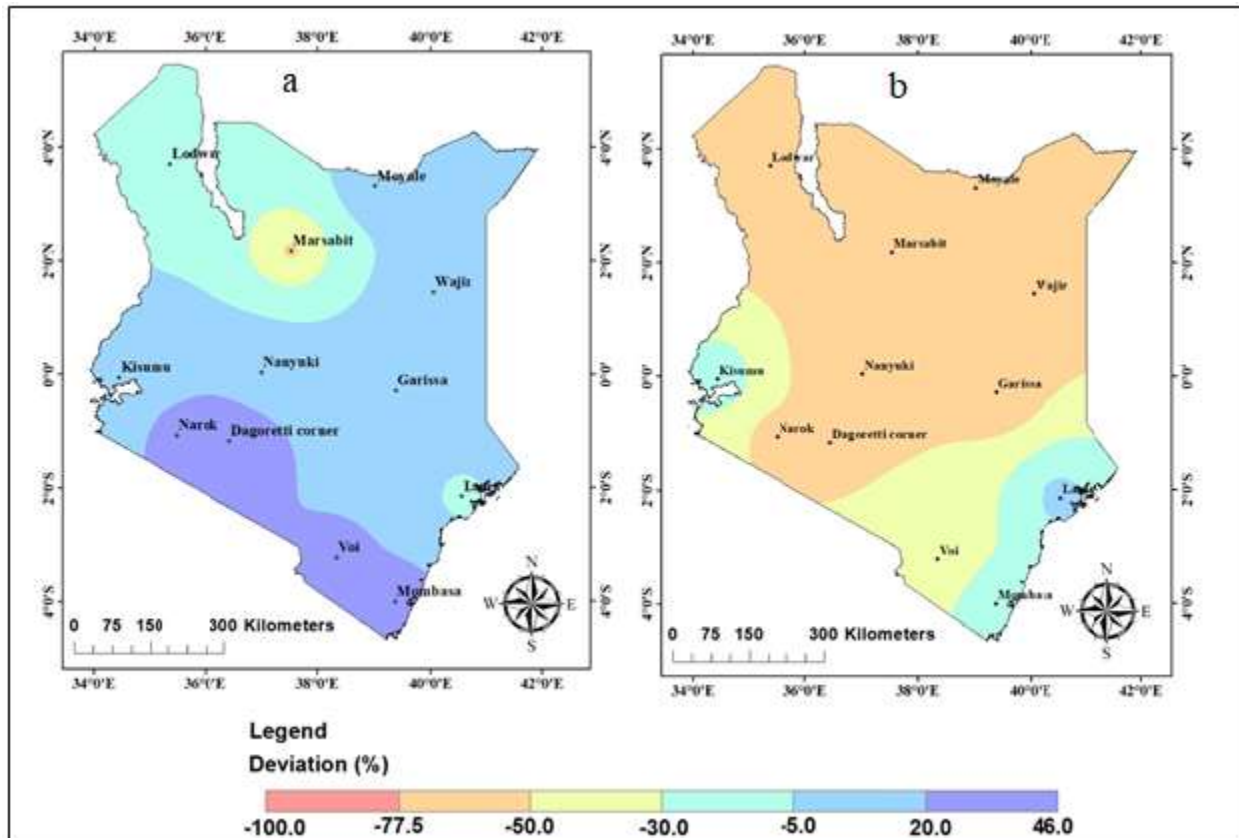


Figure 4-16: The spatial distribution of percentage deviation of MAM seasonal rainfall of 2006 and 2019 over Kenya

The findings indicate that in 2006, there was an increase in MAM rainfall despite a low prevalence of tropical cyclones. Conversely, in 2019, the MAM season had reduced precipitation compared to the long-term average for MAM seasons. Therefore, a rise in the occurrence of tropical cyclones at a certain period will have an adverse impact on the MAM season.



#### 4.4.4 The Spatial Characteristics of the Long-Term Mean of MAM Rainfall with the Seasonal Rains for MAM 2006 and 2019

**Figure 4-17** depicts the spatial coverage of the long-term mean of MAM rains, the MAM seasons of 2006 and 2019 MAM season over Kenya. These comparisons show the spatial coverage of the twelve homogeneous zones with long term mean, MAM of 2006 and MAM season of 2019, with high rain zones represented by deep blue color and low rain zones represented by brown color.

**Figure 4-17 a**, the spatial distribution of Long-term-mean MAM seasonal rainfall throughout Kenya is depicted, revealing that the majority of zones experience MAM rainfall levels over 300 mm. The average annual rainfall during the MAM season in Zones 1, 3, and 4 is below 300 mm. The seasonal precipitation in Zones 5, 6, 8, and 12 surpasses 400 mm. During the period spanning from March to May, these particular zones get a notably higher amount of precipitation compared to other zones.

**Figure 4-17 b** illustrates the spatial extent of MAM season in Kenya during the year 2006. In the year characterized by a relatively low number (3) of tropical cyclones occurring over the Southwestern Indian Ocean, the homogenous zones experienced an increase in MAM rainfall. There were adverse effects observed in only two specific zones, namely Lodwar Station in Zone 1 and Marsabit Station in Zone 11. The remaining homogenous zones surpassed their respective long-term averages.

**Figure 4-17 c** displays the regional distribution of MAM seasonal precipitation in the year 2019, revealing that 8 out of the 12 zones recorded rainfall amounts below 220 mm. The ASAL region saw a precipitation level of less than 100 mm during the designated season, rendering it one of the most adversely affected areas. Specifically, the localities of Lodwar in Zone 1, Wajir in Zone 3, Garissa in Zone 4, and Marsabit in Zone 9 were particularly impacted. Zones 5 and 6 located in the coastal region, as well as Zone 8, Zone 12, and their surrounding areas, saw precipitation above 300 mm, demonstrating a comparatively favorable performance in comparison to Arid and Semi-Arid zones.

The analysis reveals that the spatial distribution of the 2019 March-April-May seasonal rainfall indicates that a significant proportion of the country experienced precipitation levels of 220 mm or less. In contrast, the long-term average for the March-April-May season demonstrates that the majority of the country typically receives rainfall amounts equal to or exceeding 220 mm. The data

indicates that the March-April-May precipitation levels in 2019 exhibited a decline in the majority of regions within the country, resulting in a negative deviation.

In the year 2019, March-April-May season experienced a notable decrease in precipitation, with the maximum recorded rainfall ranging from 400 mm to 464 mm. In contrast to the Long Term Mean of isohyet, which ranges from 509 mm to 561 mm, there is a negative deviation of 100 mm. In a similar vein, the precipitation recorded in 2019 exhibited a smaller magnitude compared to the long-term average rainfall throughout March-April-May. Specifically, observed rainfall in 2019 varied from 25 mm to 75 mm, whereas the historical data indicates a range of 95 mm to 147 mm for the same period. The rainfall variation with the lowest value was recorded at -70 mm.

In the study, Muthoni *et al.* (2019) conducted an investigation comparing the long-term geographical and rainfall variability across Eastern and Southern Africa. The findings of this study revealed notable increases in variability over Southwestern Zambia and in the northern region of Lake Victoria. A decline in precipitation was seen in the central and southern regions of Kenya.

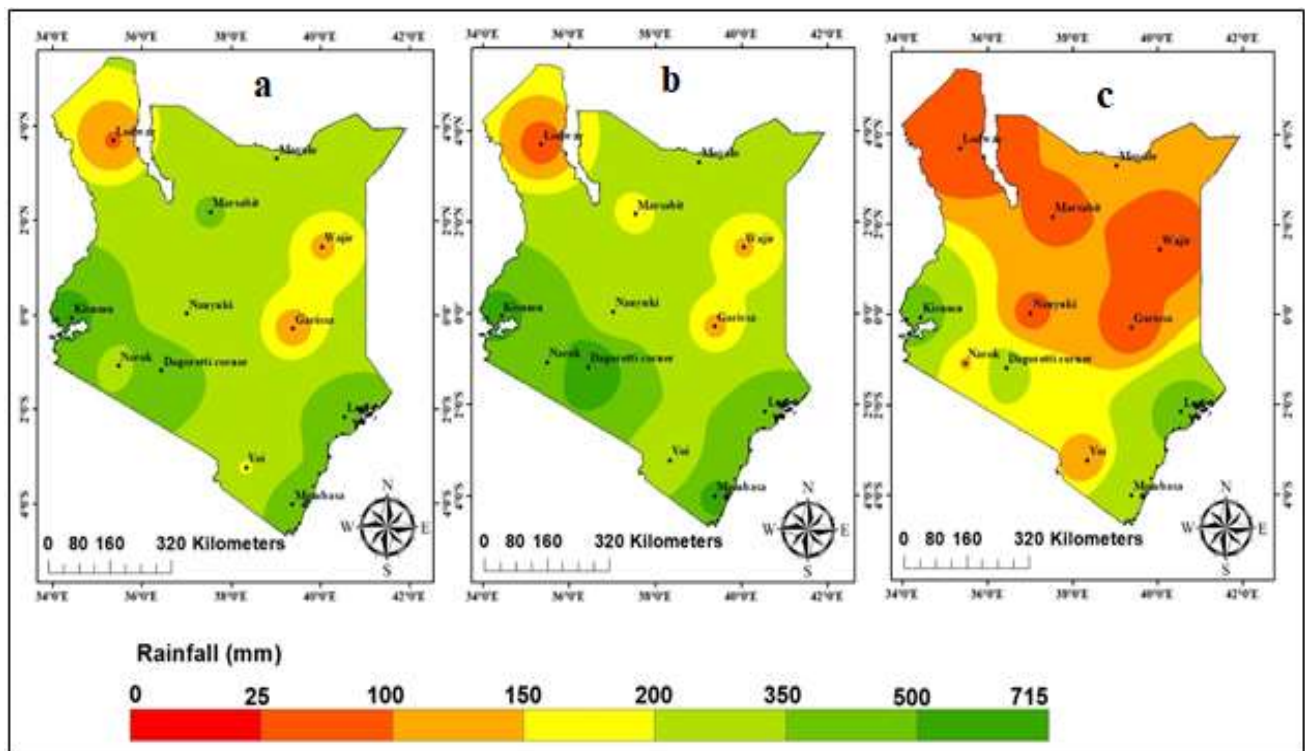


Figure 4-17: The spatial distribution of Long Term Mean of March-April-May season (1980-2019) (a), 2006 March-April-May season (b) and 2019 March-April-May season (c) of Kenya

## CHAPTER FIVE

### 5.0 CONCLUSIONS AND RECOMMENDATIONS

This chapter provides definitive conclusions and recommendations for scientists, users, and policymakers.

#### 5.1 Conclusions

This study examined the potential correlation between tropical cyclones in the Southwestern Indian Ocean and rainfall in Kenya during the long rain (MAM) season.

Data used are seasonal totals for tropical cyclone frequency over the SWIO region, from November 1979-April 2019, extracted from IBTrACS, and monthly rainfall for March-April-May seasons from 1980 to 2019 sourced from Kenya Meteorological Department.

Time series analysis and spatial distribution analysis were conducted to depict the seasonal fluctuation over a forty-year period. The significance of a trend during long rainy season (March-April-May) for all twelve zones was determined by employing the Mann-Kendall test and calculating the coefficient of variation. The third objective examined the probable relationship between the frequency of tropical cyclones with rainfall seasons of March, April, and May. This was done by presenting numerous time series on a single graph. A correlation study was performed using a Taylor Diagram. The significance was tested using a student test. The Long Term Mean was compared with the March-April-May period for the 2006 season and 2019, depending on their spatial distribution.

The March-April-May rainy season has exhibited variability over the past four decades, with the most significant impacts observed in zones classified as Arid and Semi-Arid Lands (drylands). However, overall, precipitation variation was observed across all homogeneous zones. Ten homogeneous zones were represented by the normalized values of seasonal precipitation, which were all negative and equal to 1, within the range of 12.5% to 20%. Ten zones (12.5-20%) exhibited positive standardized anomalies within the same range, whereas the two zones (7 and 12) displayed anomalies below 12%. This demonstrates that MAM seasons have been highly variable for the past four decades. In the years 1982, 1987, and 2012, significant March-April-May seasonal precipitation was documented, which coincided with a decline in the frequency of tropical cyclones over the southwestern of the Indian Ocean. In contrast, years with decreased precipitation

during the March-April-May season experienced a higher frequency of tropical cyclones. A mere 6% of the nation is habitable for agricultural purposes, as evidenced by the fact that two-thirds of the homogeneous zones (8 out of 12 zones) receive precipitation below 350 mm.

Upon conducting an examination of the temporal and spatial distributions, as well as the computation of the coefficient of variation, pertaining March-April-May rain season in Kenya spanning from 1980 to 2019, it became evident that the dryland regions of Lodwar (Zone 1), Wajir (Zone 3), Garissa (Zone 4), and Marsabit (Zone 11) experienced fluctuating and diminished precipitation. Zones in the ASAL region characterized by high Coefficient of Variation values despite receiving little precipitation. An additional relationship between coefficient variation and spatial distribution can be observed regions characterized by high seasonal rainfall exhibit low values of Coefficient of Variation, while those zones with low rainfall display high values of Coefficient Variation. The March-April-May precipitation in all homogeneous zones showed of variation of between 38% and 74%, with a Coefficient of Variation exceeding 50% in the majority of ASAL regions.

According to the Mann-Kendall test, the precipitation trends determined by March-April-May were not statistically significant, as the P-values for eleven out of twelve zones were greater than 0.1, indicating either feeble or non-changing trends. With a Kendall rank correlation (Tau) of -2.0907 and a P-value of 0.018, the seasonal precipitation at Moyale Station in zone 2 exhibited a declining trend during the March-April-May season.

Cyclone season over the Southwestern Indian Ocean commences in November and concludes in April, as illustrated by the graph. January and February are the months with the greatest frequency of cyclones. They occur mostly during the southern hemisphere summer when sea surface temperatures are relatively high as compared to other seasons. Tropical cyclone shows variability throughout the period of forty years of their season.

Kenya's seasonal precipitation decreases as a result of the heightened occurrence of tropical storms in the southwestern of the Indian Ocean. The Taylor diagram analysis revealed a negative correlation between seasonal precipitation and cyclone frequency. The Student test revealed a substantial correlation among seven out of twelve homogeneous zones. The zones with p-values below significance level of 0.05 are Zones 1, 3, 4, 7, 10, 11, and 12. This analysis proves that there

is adverse effect whenever the frequency of tropical cyclone occurs over the southwestern of the Indian Ocean as shown during 2019 March-April-May season.

By comparing March-April-May seasonal rainfall for years 2006 and 2019, which experienced the lowest or highest frequencies of tropical cyclones, one can discern the impact that the seasons had on precipitation in both instances. Percentage deviation and spatial maps across all homogeneous zones in Kenya indicate that seasonal precipitation was highest in 2006 and lowest in 2019. Dryland (soil and semi-arid) zones experienced adverse effects during the 2019 season. Seasonal precipitation was adversely affected by the increased frequency of tropical cyclones in 2019, resulting in a reduction in the amount of precipitation received during the March-April-May season. In contrast to 2019, eleven zones experienced negative seasonal rainfall deviations, while eight out of twelve zones exhibited positive deviations during the March-April-May season of 2006. The 2006 March-April-May season had enhanced rainfall as compared 2019 March-April-May season that was affected by the increased frequency of tropical cyclones in 2018/2019, as there was a more than 60% negative difference between the long-term typical March-April-May season and MAM season of 2019.

Tropical cyclone occurrence over the Southwestern of the Indian Ocean affects indirectly the performance of the main seasonal rainfall in Kenya. It adversely affects the overall rainfall received in a given season as seven zones of twelve are significantly correlated.

## **5.2 Recommendations**

### **5.2.1 To Scientists**

This study aimed to investigate the potential correlation between the heightened occurrence of tropical cyclones in the Southwestern Indian Ocean and the seasonal MAM rainfall patterns in Kenya. Researchers should investigate the impact of tropical cyclones on seasonal rainfall at various phases of development, intensities, and their specific influence on the overall seasonal rainfall patterns. Cyclones are rapidly occurring mesoscale phenomena that have a significant impact on the daily weather patterns in many regions of Kenya. Therefore, it is crucial for scholars to study their influence.

### **5.2.2 To Policymakers**

Create policies that will help in mitigation and adaptation in the region that show adversely affected with increased occurrence of cyclone over SWIO. This will aid in planning and preventing loses to livestock and crops during such period. This can be incorporate in forecasting to help warn of potential risk expect when cyclones umbers increase over SWIO.

### **5.2.3 To Users**

This information will benefit the agricultural, energy, health, tourism, and water resources sectors as it will serve as warning to the zones more vulnerable to tropical cyclones occurrence. These sectors can collaborate closely with relevant local communities to achieve optimal results through proper planning and information utilization. This can be used in short-term planning activities in various sectors for optimum utilization of the study information.

## REFERENCES

- Aditya, F., Gusmayanti, E., & Sudrajat, J. (2021). Rainfall trend analysis using Mann-Kendall and Sen's slope estimator test in West Kalimantan. *IOP Conference Series: Earth and Environmental Science*, 893(1), 012006. <https://doi.org/10.1088/1755-1315/893/1/012006>
- Ash, K. D., & Matyas, C. J. (2012). The influences of ENSO and the subtropical Indian Ocean Dipole on tropical cyclone trajectories in the southwestern Indian Ocean. *International Journal of Climatology*, 32(1), 41–56.
- Asnani, G. C., & Kinuthia, J. H. (1979). *Diurnal variation of precipitation in East Africa*. Republic of Kenya, Meteorological Department, East African Institute for Meteorological Training and Research.
- Ayugi, B. O., Tan, G., Ongoma, V., & Mafuru, K. B. (2018). Circulations Associated with Variations in Boreal Spring Rainfall over Kenya. *Earth Systems and Environment*, 2(2), 421–434. <https://doi.org/10.1007/s41748-018-0074-6>
- Baldwin, M. P., Gray, L. J., Dunkerton, T. J., Hamilton, K., Haynes, P. H., Randel, W. J., Holton, J. R., Alexander, M. J., Hirota, I., Horinouchi, T., Jones, D. B. A., Kinnersley, J. S., Marquardt, C., Sato, K., & Takahashi, M. (2001). The quasi-biennial oscillation. *Reviews of Geophysics*, 39(2), 179–229. <https://doi.org/10.1029/1999RG000073>
- Behera, S., & Yamagata, T. (2001). Subtropical SST dipole events in the Southern Indian Ocean. *Geophysical Research Letters*, 28. <https://doi.org/10.1029/2000GL011451>
- Bevans, R. (2020, January 31). *An Introduction to t Tests | Definitions, Formula and Examples*. Scribbr. <https://www.scribbr.com/statistics/t-test/>
- Borregaard, M. K., Hendrichsen, D. K., & Nachman, G. (2008). Spatial Distribution. In B. Fath (Ed.), *Encyclopedia of Ecology (Second Edition)* (pp. 589–596). Elsevier. <https://doi.org/10.1016/B978-0-444-63768-0.00659-4>

- Cervený, R. S., Bessemoulin, P., Burt, C. C., Cooper, M. A., Cunjic, Z., Dewan, A., Finch, J., Holle, R. L., Kalkstein, L., Kruger, A., Lee, T., Martínez, R., Mohapatra, M., Pattanaik, D. R., Peterson, T. C., Sheridan, S., Trewin, B., Tait, A., & Wahab, M. M. A. (2017). WMO Assessment of Weather and Climate Mortality Extremes: Lightning, Tropical Cyclones, Tornadoes, and Hail. *Weather, Climate, and Society*, 9(3), 487–497. <https://doi.org/10.1175/WCAS-D-16-0120.1>
- Chatfield, C. (2004). *The Analysis of Time Series: An Introduction*. Chapman & Hall/CRC. <https://books.google.co.ke/books?id=-i2owwEACAAJ>
- Co-efficient of Variation Meaning and How to Use It*. (n.d.). Investopedia. Retrieved November 10, 2023, from <https://www.investopedia.com/terms/c/coefficientofvariation.asp>
- Dai, A., & Wigley, T. M. L. (2000). Global patterns of ENSO-induced precipitation. *Geophysical Research Letters*, 27(9), 1283–1286. <https://doi.org/10.1029/1999GL011140>
- Deshpande, M., Singh, V., Mano Kranthi, G., Koll, R., Rongmie, E., & Kumar, U. (2021). Changing status of tropical cyclones over the north Indian Ocean. *Climate Dynamics*, 57. <https://doi.org/10.1007/s00382-021-05880-z>
- Finney, D. L., Marsham, J. H., Walker, D. P., Birch, C. E., Woodhams, B. J., Jackson, L. S., & Hardy, S. (2020). The effect of westerlies on East African rainfall and the associated role of tropical cyclones and the Madden–Julian Oscillation. *Quarterly Journal of the Royal Meteorological Society*, 146(727), 647–664. <https://doi.org/10.1002/qj.3698>
- Fitchett, J. M., & Grab, S. W. (2014). A 66-year tropical cyclone record for south-east Africa: Temporal trends in a global context. *International Journal of Climatology*, 34(13), 3604–3615. <https://doi.org/10.1002/joc.3932>



- Gitau, W., Ogallo, L., Camberlin, P., & Okoola, R. (2013). Spatial coherence and potential predictability assessment of intraseasonal statistics of wet and dry spells over Equatorial Eastern Africa. *International Journal of Climatology*, 33(12), 2690–2705. <https://doi.org/10.1002/joc.3620>
- Goldenberg, S. B., Landsea, C. W., Mestas-Nuñez, A. M., & Gray, W. M. (2001). The Recent Increase in Atlantic Hurricane Activity: Causes and Implications. *Science*, 293(5529), 474–479. <https://doi.org/10.1126/science.1060040>
- Granger, O. E. (1987). Precipitation distribution. In *Climatology* (pp. 690–697). Springer US. [https://doi.org/10.1007/0-387-30749-4\\_140](https://doi.org/10.1007/0-387-30749-4_140)
- Grove, A. T., Miles, M. R., Worthington, E. B., Doggett, H., Dasgupta, B., & Farmer, B. H. (1977). The Geography of Semi-Arid Lands [and Discussion]. *Philosophical Transactions of the Royal Society of London. Series B, Biological Sciences*, 278(962), 457–475.
- Hameed, S. N. (2018, February 26). *The Indian Ocean Dipole*. Oxford Research Encyclopedia of Climate Science. <https://doi.org/10.1093/acrefore/9780190228620.013.619>
- Henderson-Sellers, A., Zhang, H., Berz, G., Emanuel, K., Gray, W., Landsea, C., Holland, G., Lighthill, J., Shieh, S.-L., Webster, P., & McGuffie, K. (1998). Tropical Cyclones and Global Climate Change: A Post-IPCC Assessment. *Bulletin of the American Meteorological Society*, 79(1), 19–38. [https://doi.org/10.1175/1520-0477\(1998\)079<0019:TCAGCC>2.0.CO;2](https://doi.org/10.1175/1520-0477(1998)079<0019:TCAGCC>2.0.CO;2)
- Hoell, A., & Funk, C. (2013). Indo-Pacific sea surface temperature influences on failed consecutive rainy seasons over eastern Africa. *Climate Dynamics*, 43. <https://doi.org/10.1007/s00382-013-1991-6>

- Indeje, M., Semazzi, F. H. M., & Ogallo, L. J. (2000). ENSO signals in East African rainfall seasons. *International Journal of Climatology*, 20(1), 19–46. [https://doi.org/10.1002/\(SICI\)1097-0088\(200001\)20:1<19::AID-JOC449>3.0.CO;2-0](https://doi.org/10.1002/(SICI)1097-0088(200001)20:1<19::AID-JOC449>3.0.CO;2-0)
- Ingham, K., Ntarangwi, M., & Ominde, S. H. (2023, July 12). *Kenya | People, Map, Flag, Religion, Language, Capital, & Election | Britannica*. <https://www.britannica.com/place/Kenya>
- Jamal, H. (n.d.). *How to Estimate Missing Precipitation Data | Methods for Rainfall Data Estimation*. Retrieved November 10, 2023, from <https://www.aboutcivil.org/analysis-of-precipitation-data.html>
- Kai, K. H., Osima, S. E., Ismail, M. H., Waniha, P., & Omar, H. A. (2021). Assessment of the Impacts of Tropical Cyclones Idai to the Western Coastal Area and Hinterlands of the South Western Indian Ocean. *Atmospheric and Climate Sciences*, 11(4), Article 4. <https://doi.org/10.4236/acs.2021.114047>
- Kebacho, L. L. (2022). The Role of Tropical Cyclones Idai and Kenneth in Modulating Rainfall Performance of 2019 Long Rains over East Africa. *Pure and Applied Geophysics*, 179, 1387–1401. <https://doi.org/10.1007/s00024-022-02993-2>
- Kenya National Bureau of Statistics. (2019). *2019 Kenya population and housing census*.
- Khouakhi, A., Villarini, G., & Vecchi, G. A. (2017). Contribution of Tropical Cyclones to Rainfall at the Global Scale. *Journal of Climate*, 30(1), 359–372. <https://doi.org/10.1175/JCLI-D-16-0298.1>
- Kijazi, A., & Reason, C. (2005). Relationship between intraseasonal rainfall variability of coastal Tanzania and ENSO. *Theoretical and Applied Climatology*, 82, 153–176. <https://doi.org/10.1007/s00704-005-0129-0>

- Kijne, J., Barron, J., Hoff, H., Rockstroma, J., Karlberg, L., Growing, J., Wani, S. P., & Wichelns, D. (2009). *Opportunities to Increase Water Productivity in Agriculture with Special Reference to Africa and South Asia. Stockholm Environment Institute, Project Report—2009* [Monograph]. Stockholm Environment Institute. <http://oar.icrisat.org/3811/>
- Klotzbach, P. J., Wood, K. M., Schreck III, C. J., Bowen, S. G., Patricola, C. M., & Bell, M. M. (2022). Trends in Global Tropical Cyclone Activity: 1990–2021. *Geophysical Research Letters*, *49*(6), e2021GL095774. <https://doi.org/10.1029/2021GL095774>
- Knerr, I., Trachte, K., Garel, E., Huneau, F., Santoni, S., & Bendix, J. (2020). Partitioning of Large-Scale and Local-Scale Precipitation Events by Means of Spatio-Temporal Precipitation Regimes on Corsica. *Atmosphere*, *11*(4), Article 4. <https://doi.org/10.3390/atmos11040417>
- Koech, E. (2014a). *Systems associated with wet spells over Kenya during the usually dry December-February season* [Thesis, University of Nairobi]. <http://erepository.uonbi.ac.ke/handle/11295/77080>
- Koech, E. (2014b). *Systems associated with wet spells over Kenya during the usually dry December-February season* [Thesis, University of Nairobi]. <http://erepository.uonbi.ac.ke/handle/11295/77080>
- Konapala, G., Mishra, A. K., Wada, Y., & Mann, M. E. (2020). Climate change will affect global water availability through compounding changes in seasonal precipitation and evaporation. *Nature Communications*, *11*(1), Article 1. <https://doi.org/10.1038/s41467-020-16757-w>
- Kossin, J. P., Knapp, K. R., Vimont, D. J., Murnane, R. J., & Harper, B. A. (2007). A globally consistent reanalysis of hurricane variability and trends. *Geophysical Research Letters*, *34*(4). <https://doi.org/10.1029/2006GL028836>

- Kubota, H., & Wang, B. (2009). How Much Do Tropical Cyclones Affect Seasonal and Interannual Rainfall Variability over the Western North Pacific? *Journal of Climate - J CLIMATE*, 22. <https://doi.org/10.1175/2009JCLI2646.1>
- Kunze, S. (2021). Unraveling the Effects of Tropical Cyclones on Economic Sectors Worldwide: Direct and Indirect Impacts. *Environmental and Resource Economics*, 78(4), 545–569. <https://doi.org/10.1007/s10640-021-00541-5>
- Lenzen, M., Malik, A., Kenway, S., Daniels, P., Lam, K. L., & Geschke, A. (2018). Economic damage and spill-overs from a tropical cyclone. *Natural Hazards and Earth System Sciences Discussions*, 1–28. <https://doi.org/10.5194/nhess-2017-440>
- Li, J., Bao, Q., Liu, Y., Wu, G., Lei, W., He, B., Wang, X., & Li, J. (2019). Evaluation of FAMIL2 in Simulating the Climatology and Seasonal-to-Interannual Variability of Tropical Cyclone Characteristics. *Journal of Advances in Modeling Earth Systems*, 11. <https://doi.org/10.1029/2018MS001506>
- Lima, M. M., Hurduc, A., Ramos, A. M., & Trigo, R. M. (2021). The Increasing Frequency of Tropical Cyclones in the Northeastern Atlantic Sector. *Frontiers in Earth Science*, 9. <https://www.frontiersin.org/article/10.3389/feart.2021.745115>
- Marchant, R., Mumbi, C., Behera, S., & Yamagata, T. (2007). The Indian Ocean dipole – the unsung driver of climatic variability in East Africa. *African Journal of Ecology*, 45(1), 4–16. <https://doi.org/10.1111/j.1365-2028.2006.00707.x>
- Mendelsohn, R., Emanuel, K., Chonabayashi, S., & Bakkensen, L. (2012). The impact of climate change on global tropical cyclone damage. *Nature Climate Change*, 2(3), Article 3. <https://doi.org/10.1038/nclimate1357>

- Mueni, P. J. (2016). *Climate Change Impacts On Water Resources Over The Upper Tana Catchment Of Kenya* [Thesis, University Of Nairobi].  
<http://erepository.uonbi.ac.ke/handle/11295/97575>
- Mühr, B. (2019, March 27). Tropical Cyclone 18S IDAI (Africa/engl.). *Faszination Wetter*.  
<https://faszination-wetter.de/tropische-zyklone/tropical-cyclone-18s-idai-africa-engl/>
- Muthama, N., Manene, M., & Ndetei, C. (2008). Simulation of Decadal Precipitation over Nairobi in Kenya. *SQU Journal For Science*, 13, 43–54.  
<https://doi.org/10.24200/squjs.vol13iss0pp43-54>
- Muthoni, F. K., Odongo, V. O., Ochieng, J., Mugalavai, E. M., Mourice, S. K., Hoesche-Zeledon, I., Mwila, M., & Bekunda, M. (2019). Long-term spatial-temporal trends and variability of rainfall over Eastern and Southern Africa. *Theoretical and Applied Climatology*, 137(3), 1869–1882. <https://doi.org/10.1007/s00704-018-2712-1>
- Ng'ongolo, H., & Smyshlyayev, S. (2010). The statistical prediction of East African rainfalls using quasi-biennial oscillation phases information. *Natural Science*, 2, 1407–1416.  
<https://doi.org/10.4236/ns.2010.212172>
- Nhamo, G., & Chikodzi, D. (2021). *The Catastrophic Impact of Tropical Cyclone Idai in Southern Africa* (pp. 3–29). [https://doi.org/10.1007/978-3-030-72393-4\\_1](https://doi.org/10.1007/978-3-030-72393-4_1)
- Nicholson, S. E. (2017). Climate and climatic variability of rainfall over eastern Africa. *Reviews of Geophysics*, 55(3), 590–635. <https://doi.org/10.1002/2016RG000544>
- Nyakwada, W., Ogallo, L. A., & Okoola, R. E. (2009). *The Atlantic-Indian Ocean Dipole and its influence on East African seasonal rainfall*.  
<http://erepository.uonbi.ac.ke/handle/11295/28015>

- Omeny, P., Ogalo, L., Okoola, R., Hendon, H., & Wheeler, M. (2008). East African Rainfall Variability Associated with the Madden-Julian Oscillation. *J. Kenya Meteorol. Soc.*, 2.
- Ondiko, J., & Karanja, A. (2021). Spatial and Temporal Occurrence and Effects of Droughts on Crop Yields in Kenya. *OALib*, 08, 1–13. <https://doi.org/10.4236/oalib.1107354>
- Palmer, P. I., Wainwright, C. M., Dong, B., Maidment, R. I., Wheeler, K. G., Gedney, N., Hickman, J. E., Madani, N., Folwell, S. S., Abdo, G., Allan, R. P., Black, E. C. L., Feng, L., Gudoshava, M., Haines, K., Huntingford, C., Kilavi, M., Lunt, M. F., Shaaban, A., & Turner, A. G. (2023). Drivers and impacts of Eastern African rainfall variability. *Nature Reviews Earth & Environment*, 4(4), 254–270. <https://doi.org/10.1038/s43017-023-00397-x>
- Pandian, S. (2021, October 23). Time Series Analysis and Forecasting | Data-Driven Insights (Updated 2023). *Analytics Vidhya*. <https://www.analyticsvidhya.com/blog/2021/10/a-comprehensive-guide-to-time-series-analysis/>
- Pendergrass, A. G., Knutti, R., Lehner, F., Deser, C., & Sanderson, B. M. (2017). Precipitation variability increases in a warmer climate. *Scientific Reports*, 7(1), Article 1. <https://doi.org/10.1038/s41598-017-17966-y>
- Pohl, B., & Camberlin, P. (2006). Influence of the Madden–Julian Oscillation on East African rainfall: II. March–May season extremes and interannual variability. *Quarterly Journal of the Royal Meteorological Society*, 132(621), 2541–2558. <https://doi.org/10.1256/qj.05.223>
- Ratna, S. B., Cherchi, A., Osborn, T. J., Joshi, M., & Uppara, U. (2021). The Extreme Positive Indian Ocean Dipole of 2019 and Associated Indian Summer Monsoon Rainfall Response. *Geophysical Research Letters*, 48(2), e2020GL091497. <https://doi.org/10.1029/2020GL091497>

- Reason, C. J. C., & Keibel, A. (2004). Tropical Cyclone Eline and Its Unusual Penetration and Impacts over the Southern African Mainland. *Weather and Forecasting*, 19(5), 789–805. [https://doi.org/10.1175/1520-0434\(2004\)019<0789:TCEAIU>2.0.CO;2](https://doi.org/10.1175/1520-0434(2004)019<0789:TCEAIU>2.0.CO;2)
- Rwigi, S. K. (2014). *Analysis of Potential Impacts of Climate Change and Deforestation on Surface Water Yields from the Mau Forest Complex Catchments in Kenya* [Thesis, University of Nairobi]. <http://erepository.uonbi.ac.ke/handle/11295/72974>
- Sahoo, B., & Bhaskaran, P. K. (2016). Assessment on historical cyclone tracks in the Bay of Bengal, east coast of India. *International Journal of Climatology*, 36(1), 95–109. <https://doi.org/10.1002/joc.4331>
- Samrin, F., Irwana, I., Trismidianto, & Hasanah, N. (2019). Analysis of the Meteorological Condition of Tropical Cyclone Cempaka and Its Effect on Heavy Rainfall in Java Island. *IOP Conference Series: Earth and Environmental Science*, 303, 012065. <https://doi.org/10.1088/1755-1315/303/1/012065>
- Schneider, T., Bischoff, T., & Haug, G. (2014). Migrations and dynamics of the Intertropical Convergence Zone. *Nature*, 513, 45–53. <https://doi.org/10.1038/nature13636>
- Season of the Tropical Cyclones in Southern Indian Ocean, 18th Feb 2023—Kenya* | ReliefWeb. (2023, February 18). <https://reliefweb.int/report/kenya/season-tropical-cyclones-southern-indian-ocean-18th-feb-2023>
- Shanko, D., & Camberlin, P. (1998). The effects of the Southwest Indian Ocean tropical cyclones on Ethiopian drought. *International Journal of Climatology: A Journal of the Royal Meteorological Society*, 18(12), 1373–1388.
- Slingo, J., Weller, H., Hoskins, B., Berrisford, P., & Black, E. (2005). The meteorology of the Western Indian Ocean, and the influence of the East African Highlands. *Philosophical*

- Transactions of the Royal Society A: Mathematical, Physical and Engineering Sciences*, 363. <https://doi.org/10.1098/rsta.2004.1473>
- Southern Africa: Snapshot of Tropical Cyclone Freddy's Impact (February - March 2023) - Malawi* | ReliefWeb. (2023, July 21). <https://reliefweb.int/report/malawi/southern-africa-snapshot-tropical-cyclone-freddys-impact-february-march-2023>
- Taylor, K. (2001). Summarizing multiple aspects of model performance in a single diagram. *Journal of Geophysical Research*, 106, 7183–7192. <https://doi.org/10.1029/2000JD900719>
- Thornton, P. K., Ericksen, P. J., Herrero, M., & Challinor, A. J. (2014). Climate variability and vulnerability to climate change: A review. *Global Change Biology*, 20(11), 3313–3328. <https://doi.org/10.1111/gcb.12581>
- Time Series Analysis: Definition, Types, Techniques, and When It's Used*. (n.d.). Tableau. Retrieved July 19, 2022, from <https://www.tableau.com/learn/articles/time-series-analysis>
- Tyson, P. D., Garstang, M., & Swap, R. (1996). Large-Scale Recirculation of Air over Southern Africa. *Journal of Applied Meteorology and Climatology*, 35(12), 2218–2236. [https://doi.org/10.1175/1520-0450\(1996\)035<2218:LSROAO>2.0.CO;2](https://doi.org/10.1175/1520-0450(1996)035<2218:LSROAO>2.0.CO;2)
- Uhe, P., Philip, S., Kew, S., Shah, K., Kimutai, J., Mwangi, E., van Oldenborgh, G. J., Singh, R., Arrighi, J., Jjemba, E., Cullen, H., & Otto, F. (2018). Attributing drivers of the 2016 Kenyan drought. *International Journal of Climatology*, 38(S1), e554–e568. <https://doi.org/10.1002/joc.5389>
- Vellinga, M., & Milton, S. F. (2018). Drivers of interannual variability of the East African “Long Rains.” *Quarterly Journal of the Royal Meteorological Society*, 144(712), 861–876. <https://doi.org/10.1002/qj.3263>



- Villarini, G., & Denniston, R. (2015). Contribution of tropical cyclones to extreme rainfall in Australia. *International Journal of Climatology*, 36. <https://doi.org/10.1002/joc.4393>
- Wakachala, F., Shilenje, Z. W., Nguyo, J., Shaka, S., Apondo, W., Rehmani, M. I. A., & Rehmani, M. I. A. (2015). Statistical Patterns of Rainfall Variability in the Great Rift Valley of Kenya. *Journal of Environmental and Agricultural Sciences* 2313-8629, 5, 17–26.
- Wang, C., & Wu, L. (2012). Tropical Cyclone Intensity Change in the Western North Pacific: Downscaling from IPCC AR4 Experiments. *気象集誌 第2輯*, 90(2), 223–233. <https://doi.org/10.2151/jmsj.2012-205>
- Wing, A. A., Sobel, A. H., & Camargo, S. J. (2007). Relationship between the potential and actual intensities of tropical cyclones on interannual time scales. *Geophysical Research Letters*, 34(8). <https://doi.org/10.1029/2006GL028581>
- Yang, W., Seager, R., Cane, M. A., & Lyon, B. (2015). The Annual Cycle of East African Precipitation. *Journal of Climate*, 28(6), 2385–2404. <https://doi.org/10.1175/JCLI-D-14-00484.1>
- Yoshida, K., & Itoh, H. (2012). Indirect Effects of Tropical Cyclones on Heavy Rainfall Events in Kyushu, Japan, During the Baiu Season. *Journal of the Meteorological Society of Japan. Ser. II*, 90, 377–401. <https://doi.org/10.2151/jmsj.2012-303>
- Zhang, W., Furtado, K., Wu, P., Zhou, T., Chadwick, R., Marzin, C., Rostron, J., & Sexton, D. (2021). Increasing precipitation variability on daily-to-multiyear time scales in a warmer world. *Science Advances*, 7(31), eabf8021. <https://doi.org/10.1126/sciadv.abf8021>
- Zhu, L., & Quiring, S. M. (2022). Exposure to precipitation from tropical cyclones has increased over the continental United States from 1948 to 2019. *Communications Earth & Environment*, 3(1), Article 1. <https://doi.org/10.1038/s43247-022-00639-8>

Zinke, J., Pfeiffer, M., Timm, O., Dullo, W.-C., & Brummer, G. J. A. (2009). Western Indian Ocean marine and terrestrial records of climate variability: A review and new concepts on land–ocean interactions since AD 1660. *International Journal of Earth Sciences*, 98, 115–133.

# APPENDIX

Single mass curves for homogeneous zones

